

Boosting In-Context Learning in LLMs Through the Lens of Classical Supervised Learning

Korel Gundem¹, Juncheng Dong², Dennis Zhang³, Vahid Tarokh², Zhengling Qi¹

¹The George Washington University, Washington, DC

²Duke University, Durham, NC

³Olin School of Business, Washington University in St. Louis, St. Louis, MO

June 12, 2025

Abstract

In-Context Learning (ICL) allows Large Language Models (LLM) to adapt to new tasks with just a few examples, but their predictions often suffer from systematic biases, leading to unstable performances in classification. While calibration techniques are proposed to mitigate these biases, we show that, in the logit space, many of these methods are equivalent to merely shifting the LLM’s decision boundary without having the ability to alter its orientation. This proves inadequate when biases cause the LLM to be severely misdirected. To address these limitations and provide a unifying framework, we propose Supervised Calibration (SC), a loss-minimization based framework, which learns an optimal, per-class affine transformation of LLM’s predictive probabilities in the logit space without requiring external data beyond the context. By using a more expressive functional class, SC not only subsumes many existing calibration methods in ICL as special cases but also enables the ability of altering and even completely reversing the orientation of the LLM’s decision boundary. Furthermore, SC’s loss-based nature facilitates the seamless integration of two purpose-built regularization techniques—context-invariance and directional trust-region regularizers. The former is designed to tackle the instability issue in ICL, while the latter is to control the degree of calibration. Finally, SC delivers state-of-the-art performance over calibration baselines in the 4-shot, 8-shot, and 16-shot settings across all nine datasets for Mistral-7B-Instruct-v0.3, Llama-2-7B-chat, and Qwen2-7B-Instruct.

1 Introduction

State-of-the-art LLMs exhibit a striking *in-context learning* (ICL) capability: with only a handful of input–label exemplars, they generalize to unseen queries almost as if they had been fine-tuned, thus functioning as highly sample-efficient few-shot learners [2, 13]. However, a growing body of evidence shows that ICL performance can be brittle—sometimes

systematically biased—with respect to seemingly innocent design choices such as template wording [17], verbaliser selection [7], and the particular demonstrations given [12]. These biases and sensitivity of ICL pose a practical barrier to developing applications that are both adaptable and robust.

Motivated by this, extensive research has been conducted to develop calibration approaches to address such a challenge for classification problems in ICL. The majority of calibration methods fall under label-marginal-based calibration (LM) [42, 8, 5, 44]. These methods first estimate the LLM’s probability for each label given the context alone via various approaches. They then discount the predictive probabilities of the LLM for the labels that are over-represented and boost those that are under-represented. See detailed discussion in the later sections.

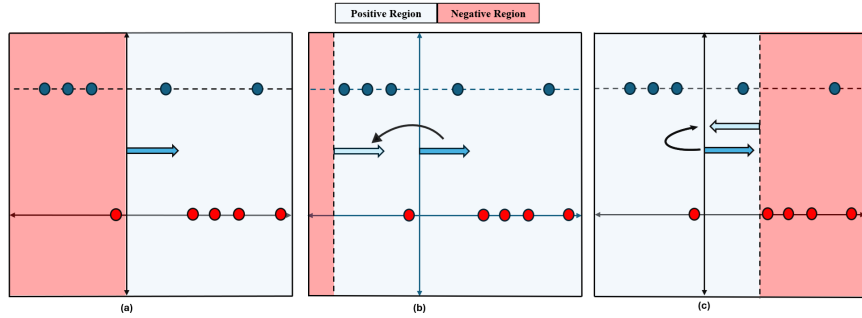


Figure 1: Comparison of ICL prediction strategies, where the x-axis represents the LLM’s raw logits (log-odds). **(a)** *Base LLM* (accuracy: 30%): The model predicts class 1 when $\text{logit} > 0$. **(b)** *Label Marginal Calibration* (accuracy: 50%): These methods only shift the decision boundary, limiting correction when base LLM is systematically wrong. **(c)** *Supervised Calibration* (accuracy: 80%): SC can shift and flip the decision boundary of the base LLM, resulting in a significant improvement.

Despite the empirical success of these methods, their ability of correcting the predictive probabilities of the LLM via its internal estimated prior is limited. Specifically, we show in Section 3.4 that the underlying idea of these methods is equivalent to optimally shifting the decision threshold of the base LLM. Hence, they are inherently incapable of altering or reversing the orientation of the decision boundary. This becomes problematic when the base LLM performs poorly. To further illustrate this limitation, consider a binary classification problem in Figure 1 (a), where the base LLM only achieves 30% accuracy. Since LM methods can only shift the decision threshold, their maximum improvement over the base LLM is capped, only achieving the level of random guessing as seen in Figure 1 (b). One may expect that such an issue becomes more common and severe in the multiclass classification, where distinguishing among a larger number of labels is inherently more difficult. For instance, on the SST-5 dataset, the average accuracy across three representative LLMs is

only 22%, highlighting the severity of this challenge. This limitation motivates the need for a more principled calibration framework—one that is capable of correcting severely misaligned LLM predictions when necessary (e.g., by reversing the decision direction), and that subsumes existing methods as special cases while remaining both theoretically grounded and practically robust.

To achieve this goal, we introduce Supervised Calibration (SC), which is motivated by conceptualizing existing approaches as learning a calibrated classifier: they take a LLM’s logits as input features and subsequently optimize a bias term to shift these logits. However, this shift only corresponds to moving the LLM’s decision boundary to maximize the predictive accuracy illustrated in Figure 1 (b). Therefore, to enable more comprehensive adjustments—specifically, the ability to alter or reverse the orientation of the LLM’s decision boundary—the proposed SC leverages the paradigm of loss-function-based classification and optimize both the bias and the scaling factor jointly. Our approach begins by generating a surrogate dataset, removing the necessity of external dataset beyond the given context. From this surrogate data, we extract features in the form of logits derived from the base LLM’s output probabilities. Then we employ these features, paired with their corresponding true labels to train a standard classifier, which learns not only an optimal bias term but also an optimal rescaling factor. Critically, the concurrent optimization of this rescaling factor empowers our approach to reverse the LLM’s decision boundary when advantageous (as illustrated in Figure 1 (c)). Moreover, the loss-minimization framework underpinning SC inherently supports the integration of regularization techniques designed for addressing the common problems in ICL and calibration. In this context, we propose a novel context-invariance regularizer for addressing the instability issue in ICL and a directional trust-region regularizer for controlling the degree of calibration. From a statistical viewpoint, these characteristics allow SC to pursue a balance regarding to the bias-variance trade-off. While SC’s flexibility targets a reduction in approximation error over LM methods, its regularization components actively constrain variance—an essential consideration within the data-scarce ICL paradigm. Collectively, SC delivers an adaptable, stable, and theoretically grounded framework that improves LLMs’ classification quality in few-shot settings, enabling fairer and more socially impactful applications as a result. Experimental results demonstrate that SC consistently outperforms existing calibration methods across a broad range of tasks, significantly enhancing the predictive performance of three distinct LLMs evaluated on nine inference datasets. For example, the performance of SC is striking on the SST-5 dataset with the Qwen model (8-shot setting), where it significantly outperforms baseline methods with accuracy from 25% (baselines) to 44%. This notable boost is directly attributable to its learned negative scaling factor which re-orientes the base LLM decision boundary in this multiclass classification task. See Figure 4 for more details.

Our main contributions are summarized as follows: Firstly, we propose Supervised Calibration, which adopts loss minimization framework from classical supervised learning and calibrates ICL via learning optimal bias and scaling factors, enabling not only shifting but also altering the orientation of the base LLM decision boundary; Secondly, we integrate

the context-invariance and directional trust region regularizations in SC, enhancing the stability of ICL and controlling the degree of the calibration respectively; Thirdly, we provide a theoretical intuition behind SC and its generalization over the LM methods; Lastly, we conduct extensive empirical studies to demonstrate the state-of-the-art performance of SC over several existing calibration baselines. We have released the code to facilitate reproducibility.¹

2 Related work

Diagnosing biases and calibration via Label Marginal A seminal study by Zhao et al. [42] identified three primary ICL biases—majority-label bias, recency bias, and common-token bias—and introduced **Contextual Calibration (CC)**, a method that adjusts conditional probabilities by normalizing against outputs from content-free prompts. Subsequently, Holtzman et al. [8] observed that superficially distinct responses compete for probability mass, resulting in a degraded performance. Therefore, they proposed **DCPMI**, which recalibrates logits based on domain-conditional pointwise mutual information. Recent studies have uncovered additional sources of instability in ICL, including feature bias [27], positional biases within multiple-choice prompts [33, 21, 43], and domain-label biases [5]. Each study paired the diagnosis of a specific bias with a corresponding lightweight calibration strategy. For instance, **Domain-Context Calibration (DC)** proposed correcting predictions by averaging label distributions over random in-domain strings [5]. More recently, Zhou et al. [44] proposed **Batch Calibration (BC)**, which estimates a contextual prior from unlabeled inference-time mini-batches and adjusting each example’s prediction probability accordingly. While these LM methods show empirical improvements, they are susceptible to failure when the base LLM substantially misaligned with the downstream task as they are unable to alter the LLM’s decision direction. This motivates exploring calibration frameworks with greater flexibility.

Calibration via centroids A parallel line of work mitigates in-context biases by replacing the standard decision rule with centroid-based classification. Han et al. [6] proposed **Prototypical Calibration**, which models output probability vectors using Gaussian mixtures and assigns labels based on cluster likelihood, improving robustness to prompt variation and class imbalance. Similarly, Cho et al. [3] introduced **Hidden Calibration**, which operates in the model’s latent space by computing class centroids over hidden states and classifying based on proximity. Although these methods show empirical performance gains, they rely on additional data beyond the in-context examples, which may not always be available or compatible with the ICL setting.

¹The code repository: <https://github.com/gundemkorel/ICL>

3 Supervised Calibration

3.1 Background

Consider an n -class classification task with label verbaliser set $\mathcal{Y} = \{y_0, \dots, y_{n-1}\}$ and query space \mathcal{X} . In few-shot in-context learning (ICL), the context C_k is constructed by concatenating k input-label exemplars $(x^{(i)}, y^{(i)})$ formatted via a template function T such that $C_k = \text{Concat}(T(x^{(1)}, y^{(1)}), \dots, T(x^{(k)}, y^{(k)}))$. Then given the context of k -shots and a testing query $x \in \mathcal{X}$, the LLM predicts a label via computing

$$\hat{y} \in \arg \max_{y \in \mathcal{Y}} P_{\text{LLM}}(y \mid x, C_k).$$

While ICL offers an appealing alternative to the gradient-based fine-tuning by allowing LLMs to adapt to new tasks via only a handful of in-prompt demonstrations, the resulting posterior distribution $P_{\text{LLM}}(y \mid x, C_k)$ is often distorted by some systematic biases. Such biases inherent in ICL often stems from context examples, their order, formatting, or verbalizer choices, which makes $P_{\text{LLM}}(y \mid x, C_k)$ significantly diverge from ground-truth posterior $P^*(y|x)$. Therefore, the objective of calibration is to refine LLM’s predictive probabilities $P_{\text{LLM}}(\cdot \mid x, C_k)$ to aligns with $P^*(y|x)$.

Existing approaches are mainly focused on correcting the prior distribution of the label via estimating the LLM’s internal prior given the context. Despite their successes, one can show that these approaches boils down to merely shifting the LLM’s decision boundary, lacking the ability to alter an LLM’s orientation. This limitation turns out to be essential especially in multi-class classification, where an LLM can easily make persistent mistakes. See Figure 1. Therefore, to further reduce the biases and align with $P^*(y \mid x)$ in such cases of substantial misorientation, we develop a more principle calibration called Supervised Calibration introduced below.

3.2 Our proposal

To begin with, we assume the k context examples $(x^{(i)}, y^{(i)})_{i=1}^k \stackrel{\text{i.i.d.}}{\sim} P^*$. Due to the aforementioned biases, the LLM’s posterior $P_{\text{LLM}}(y \mid x, C_k)$ can deviate notably from the truth $P^*(y \mid x)$. In particular, we measure their deviation via the Kullback–Leibler (KL) divergence defined as

$$\mathbb{E}_{x \sim P^*} [D_{\text{KL}}(P^*(\cdot \mid x) \parallel P_{\text{LLM}}(\cdot \mid x, C_k))],$$

where $D_{\text{KL}}(P \parallel Q) = \sum_{y \in \mathcal{Y}} P(y) \log \frac{P(y)}{Q(y)}$ for some probability measures P and Q . Let Δ^n be the probability simplex over \mathcal{Y} . Then to correct for this, we seek a vector-valued calibration function $f^* : \Delta^n \rightarrow \Delta^n$, chosen from a prescribed class \mathcal{F} , such that when

applied to the vector of LLM’s predictive probabilities, it minimizes the KL-divergence, i.e.,

$$\begin{aligned} f^* &= \arg \min_{f \in \mathcal{F}} \mathbb{E}_{x \sim P^*(x)} [D_{\text{KL}}(P^*(\cdot | x) \| f(P_{\text{LLM}}(\cdot | x, C_k)))] \\ &= \arg \min_{f \in \mathcal{F}} -\mathbb{E}_{(x,y) \sim P^*} [\log(f_y(P_{\text{LLM}}(\cdot | x, C_k)))] , \end{aligned} \quad (1)$$

where f_y is the y^{th} -coordinate projection of f . Note that as long as \mathcal{F} contains the identity map, applying f^* enhances the fidelity of P_{LLM} .

To find f^* , we highlight two key challenges. Firstly, since our method is post-hoc, choosing an effective \mathcal{F} operating solely on the base LLM predictive probabilities is essential. Secondly, there is no external data sampled from P^* to approximate the objective function in Equation (1).

3.2.1 Affine-logit approximation and leave-subset-out strategy

To select an appropriate function class \mathcal{F} , we only need to consider f defined over the log-odds of the predictive probabilities against a reference group (class 0 in this paper), since the logistic function is bijective. Specifically, denote the logits given by the base LLM as

$$\mathbf{m}(x; C_k) = \left(m_c(x; C_k) \triangleq \log \frac{P_{\text{LLM}}(y = c | x, C_k)}{P_{\text{LLM}}(y = 0 | x, C_k)} \right)_{c=1}^{n-1}.$$

Then, instead, we aim to choose the transformed function class $\tilde{\mathcal{F}} = \{f : \mathbb{R}^{n-1} \rightarrow \Delta^n\}$ for calibration. To facilitate it, notice that

$$P^*(y | x) = \frac{P^*(x | y)P^*(y)}{P^*(x)} \propto P_{\text{LLM}}(y | x, C_k) \frac{P^*(x | y)}{P_{\text{LLM}}(x | y, C_k)} \frac{P^*(y)}{P_{\text{LLM}}(y | C_k)} \quad (2)$$

$$\triangleq P_{\text{LLM}}(y | x, C_k) h(x, y, C_k), \quad (3)$$

which implies that

$$L_c^*(x) = m_c(x; C_k) + \underbrace{\log \left(\frac{P^*(x|c)P_{\text{LLM}}(x|0, C_k)}{P^*(x|0)P_{\text{LLM}}(x|c, C_k)} \right)}_{\text{Class Conditional Shift}} + \underbrace{\log \left(\frac{P^*(c)P_{\text{LLM}}(0|C_k)}{P^*(0)P_{\text{LLM}}(c|C_k)} \right)}_{\text{Label Marginal Shift}}, \quad (4)$$

$\underbrace{\hspace{10em}}_{\log(h(x,c,C_k)/h(x,0,C_k))}$

where $L_c^*(x) = \log(P^*(c|x)/P^*(0|x))$ is the true logit for class c . Thus, the primary challenge of choosing \mathcal{F} lies in approximating the unknown correction term $\log(h(x, c, C_k)/h(x, 0, C_k))$. Since we only have access to the LLM’s output logits $\mathbf{m}(x; C_k)$, we propose to approximate $\{L_c^*(x)\}_{c=1}^{n-1}$ via an affine transformation of $\{m_c(x; C_k)\}_{c=1}^{n-1}$. In particular, our working model $L_c(x; \boldsymbol{\theta}_c^k)$ is

$$L_c(x; \boldsymbol{\theta}_c^k) = w_c^k m_c(x; C_k) + b_c^k, \quad c = 1, \dots, n-1, \quad (5)$$

where $\theta_c^k = (b_c^k, w_c^k)$ are calibration parameters associated with class c and the context size k . This affine structure directly targets the two primary sources of discrepancies between true and LLM logits: class-conditional shift and label marginal shift as illustrated in Equation (4). Specifically, by rearranging Equation (5) as $L_c(x; \theta_c^k) = m_c(x; C_k) + [(w_c^k - 1)m_c(x; C_k) + b_c^k]$, we see that the term $(w_c^k - 1)m_c(x; C_k) + b_c^k$ serves as our learned approximation to the true correction term $\log(h(x, c, C_k)/h(x, 0, C_k))$. Within this learned correction, the intercept b_c^k primarily addresses the query-independent "Label Marginal Shift" component from Equation (4), compensating for discrepancies in label priors. The query-dependent term $(w_c^k - 1)m_c(x; C_k)$ targets the "Class Conditional Shift" by allowing the slope w_c^k to rescale the LLM's original logit $m_c(x; C_k)$.

Furthermore, w_c^k enables the reorientation of the LLM's decision boundary. For instance, a negative w_c^k inverts the LLM's initial assessment for a class relative to the reference, effectively correcting its predictive direction as illustrated in Figures 1 (c) and 4. This is a vital capability that methods merely learning a bias (i.e., fixing $w_c^k = 1$) lack. As detailed in Section 3.4, our framework not only unifies but also generalizes several recent ICL calibration techniques. Finally, it naturally encompasses the base LLM's original predictions as a special case when $b_c^k = 0$ and $w_c^k = 1$ for all c .

In terms of learning the parameters, if an external calibration dataset $\{(x^{(j)}, y^{(j)})\}_{j=1}^{N_{cal}}$ is provided, we first compute the LLM's logits $\mathbf{m}(x^{(j)}; C_k)$ for each $x^{(j)}$. Then based on Equation (1), we estimate the parameters via minimizing the negative log-likelihood, i.e.,

$$\hat{\theta}^k = \arg \min_{\theta^k} \{\mathbb{L}_k(\theta^k) \triangleq - \sum_{j=1}^{N_{cal}} \log f_{y^{(j)}}(\mathbf{m}(x^{(j)}; C_k); \theta^k)\}, \quad (6)$$

where $\theta^k = \{\theta_c^k\}_{c=1}^{n-1}$ and $f_c(\mathbf{m}(x^{(j)}; C_k); \theta^k) = \frac{\mathbf{1}_{\{c>0\}} \exp(L_c(x; \theta_c^k)) + \mathbf{1}_{\{c=0\}}}{1 + \sum_{i=1}^{n-1} \exp(L_i(x; \theta_i^k))}$.

This optimization problem is equivalent to standard multi-class logistic regression using the model logits m_c as input features. However, there is no external calibration dataset available beyond C_k . Therefore, we propose generating surrogate training data directly from the demonstration context C_k via a leave-subset-out strategy. Specifically, we first select a context size i such that $i < k$. We then construct the surrogate training dataset \mathcal{T}_i using Algorithm 1 in Appendix E, as illustrated in Figure 2. Finally, we estimate calibration parameters $\hat{\theta}^i$ via minimizing \mathbb{L}_i under \mathcal{T}_i . Note that this method can be applied across multiple context sizes i , enabling ensembling extensions of $\{\hat{\theta}^i\}_{i \in I}$ to construct a final estimator for calibration.

3.2.2 Context invariance and directional trust region

In the following subsection, we fix the context size $i \in I$ and introduce some enhancement on the proposed method. Note that our surrogate data generation process exposes a well-known limitation of ICL, its sensitivity to the composition and ordering of the context. Specifically,

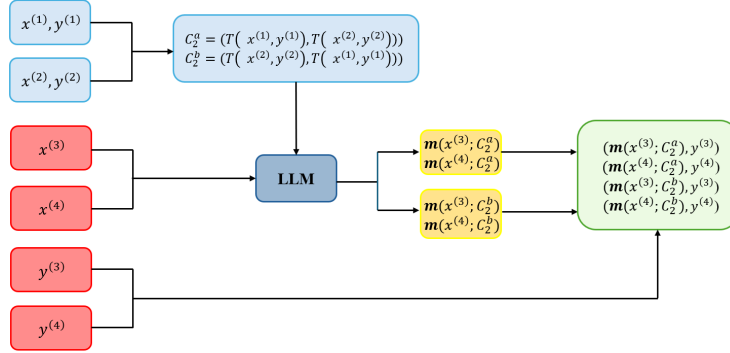


Figure 2: Illustration of surrogate data generation for $k = 4$ and $i = 2$, depicting two distinct instantiations of the context $C_2 \subset C_4$, as described in Algorithm 1. Each context C_2^a and C_2^b (shown in blue) is constructed from different orderings of two examples. The remaining examples $R_2 = C_4 \setminus C_2$ (shown in red) are passed to the LLM using each context, and the resulting logits $\mathbf{m}(x; C_2)$ are paired with their known labels to produce calibration data. Aggregating across such variations enables context-diverse surrogate training.

a single query pair (x, y) is evaluated using multiple different sub-contexts C_i , yielding potentially different logits $\mathbf{m}(x; C_i)$ and label prediction for the same ground truth label y . In essence, an effective calibration method should mitigate this sensitivity, leading to more stable predictions. This motivates incorporating a mechanism to encourage context invariance in the calibrated predictions. To achieve this, we propose augmenting the standard MLE objective (Eq. (6)) with a context-invariance regularization term. Specifically, let $C_i^{(a)}$ and $C_i^{(b)}$ be any two distinct contexts of size i drawn from C_k for evaluating the same query (x, y) in the surrogate data. We aim for the calibrated distributions $\mathbf{f}(\mathbf{m}(x^{(j)}; C_i^{(a)}); \boldsymbol{\theta}^i)$ and $\mathbf{f}(\mathbf{m}(x^{(j)}; C_i^{(b)}); \boldsymbol{\theta}^i)$, to be similar. To enforce this similarity, we utilize the symmetric cross-entropy between these two calibrated distributions as a regularizer defined as

$$L_{\text{sym}}(\boldsymbol{\theta}^i, x, C_i^{(a)}, C_i^{(b)}) = H(\mathbf{f}(\mathbf{m}(x^{(j)}; C_i^{(a)}); \boldsymbol{\theta}^i), \mathbf{f}(\mathbf{m}(x^{(j)}; C_i^{(b)}); \boldsymbol{\theta}^i)),$$

where $H(P, Q) \triangleq -\sum_{c=0}^{n-1} (P_c \log Q_c + Q_c \log P_c)$. This loss term measures the divergence between the two distributions induced by different contexts, penalizing differences in both directions. Then the overall context-invariance penalty is defined by averaging L_{sym} over all possible pairs of contexts associated with each x .

$$\text{InvPenalty}(\boldsymbol{\theta}^i) = \sum_x \sum_{\{C_i^{(a)}, C_i^{(b)}\}} L_{\text{sym}}(\boldsymbol{\theta}^i, x, C_i^{(a)}, C_i^{(b)}). \quad (7)$$

The full expression of InvPenalty is given in Equation (14) of Appendix D.

On top of ensuring context-invariance, a well-established calibration approach should also take into account the different scenarios induced by the base LLM’s reliability and the size of the context. In particular, strong base LLMs warrant minimal adjustment, while weak ones require more aggressive correction—yet limited examples can mislead both cases, risking overfitting or under-correction.

To balance it, we regularize the calibration by introducing a *directional trust region* that restricts parameter updates to remain aligned with the base LLM’s logit. Specifically, we constrain the average cosine similarity between each parameter vector $\theta_c^i = [b_c^i, w_c^i]^\top$ and the identity direction $v = [0, 1]^\top$, which corresponds to the base LLM via

$$\frac{1}{n-1} \sum_{c=1}^{n-1} \frac{(\theta_c^i)^\top v}{\|\theta_c^i\|_2} \geq \tau,$$

where $\|\cdot\|_2$ refers to ℓ_2 -norm and $\tau \in [0, 1]$ modulates the trust: large τ encourages minor scaling adjustments (exploitation), while smaller values permit broader corrections (exploration). This mirrors trust-region principles in policy optimization (e.g., TRPO [24]), adapting model updates based on the confidence in prior predictions.

3.3 Full algorithm

The final optimization combines this trust constraint with the likelihood loss and a context-invariance regularizer:

$$\begin{aligned} \min_{\theta^i} \quad & \sum_{(\mathbf{m}^{(l)}, y^{(l)}) \in \mathcal{T}_i} -\log f_{y^{(l)}}(\mathbf{m}^{(l)}; \theta^i) + \lambda_{\text{inv}} \text{InvPenalty}(\theta^i) \\ \text{s.t.} \quad & \frac{1}{n-1} \sum_{c=1}^{n-1} \frac{(\theta_c^i)^\top v}{\|\theta_c^i\|_2} \geq \tau, \end{aligned} \tag{8}$$

where $\lambda_{\text{inv}} > 0$ is a hyperparameter controlling the strength of the context-invariance penalty. To solve this optimization problem, we used *SciPy*’s `trust-constr` algorithm, a trust-region method designed for constrained optimization. This optimization can be carried out independently for each $i \in I \triangleq \{1, \dots, k-1\}$, resulting in a set of calibration models $\{\hat{\theta}^i\}_{i \in I}$, each specialized for a particular context length. Additionally, at inference, any sub-context C_i can be used to extract logits for a given size i . This paves the way for a *two-level ensembling strategy* to enhance robustness by aggregating predictions across both multiple context lengths and diverse sub-context samples.

Specifically, we train multiple affine-logit models $\{\hat{\theta}^i\}_{i \in I}$ using training sets with different sizes of the context. Then, at inference time, given a test query x_{test} , we first draw $\{C_i^{(j)}\}_{j \in \mathcal{M}_i}$ from C_k for every $i \in I$, where I and \mathcal{M}_i are user-defined index sets with size $|\mathcal{M}_i|$ and $|I|$. Then we perform *intra-size* and *inter-size* ensembling by averaging the calibrated predictions over $\{C_i^{(j)}\}_{j \in \mathcal{M}_i}$ and across all context sizes $i \in I$ and output the

predictive probability of SC for x_{test} as

$$\hat{\mathbf{p}}_{\text{SC}}(x_{\text{test}}) = \frac{1}{|I|} \sum_{i \in I} \frac{1}{|\mathcal{M}_i|} \sum_{j \in \mathcal{M}_i} \mathbf{f}(\mathbf{m}(x_{\text{test}}; C_i^{(j)}); \hat{\boldsymbol{\theta}}^i). \quad (9)$$

The final predicted label is $\hat{y}_{\text{SC}} \in \arg \max_{y \in \mathcal{Y}} [\hat{\mathbf{p}}_{\text{SC}}]_c$. Overall, this ensembling procedure approximates marginalization over plausible sub-contexts and lengths, significantly improving calibration stability and accuracy. The full algorithm of SC is summarized in Table 2 of Appendix F.

3.4 Connections to prior work and theoretical insight

In this section, we show the connection of the proposed SC with the existing LM methods and provide a principle approach to theoretically understand these methods from the perspective of supervised learning. Specifically, LM methods rely on one core assumption.

Assumption 1 *The correction term $h(x, y, C_k) \propto \frac{1}{P_{\text{LLM}}(y|C_k)}$.*

Under Assumption 1, by a similar derivation in Section 3.2.1, we can show that LM methods are equivalent to assuming

$$L_c^*(x) = m_c(x; C_k) + B_c(C_k), \quad c = 1, \dots, n-1, \quad (10)$$

where $B_c(C_k) = -\log[P_{\text{LLM}}(c|C_k)/P_{\text{LLM}}(0|C_k)]$. Therefore, they focus on optimally shifting the decision threshold of the base LLM via estimating $P_{\text{LLM}}(y|C_k)$, which thus gives an estimator for $B_c(C_k)$. We summarize the existing approaches of estimating $P_{\text{LLM}}(y|C_k)$ in Table 2 of Appendix D. However, Assumption 1 can be easily violated in practice, causing model mis-specification error.

Instead of imposing Assumption 1, we propose to understand existing LM methods from the perspective of function approximation in the supervised learning. In this case, LM methods basically assume a working model (10). In contrast, the proposed SC considers a strictly larger working model:

$$L_c(x; \boldsymbol{\theta}_c^k) = w_c^k m_c(x; C_k) + b_c^k, \quad c = 1, \dots, n-1.$$

This offers a principle framework to compare SC with LM methods and indeed shows that SC generalizes existing LM methods.

Furthermore, within this framework, we analyze these methods via statistical learning theory. Consider a dataset $\mathcal{T} = \{(x^{(j)}, y^{(j)})\}_{j=1}^N$ of size N , and denote by $\hat{f} := f_{\hat{\boldsymbol{\theta}}^k}$ the solution minimizing $\mathbb{L}_k(\boldsymbol{\theta}^k)$ under \mathcal{T} . Let \mathcal{R}^* denote the Bayes risk and $\mathcal{R}(\hat{f})$ the 0-1 risk of \hat{f} . Then, under standard regularity conditions, the excess risk of SC satisfies, with high probability:

$$\underbrace{\mathcal{R}(\hat{f}) - \mathcal{R}^*}_{\text{excess risk}} \lesssim \underbrace{\sqrt{D_{\text{KL}}(P^* \| f^*) - D_{\text{KL}}(P^* \| P^*)}}_{\text{approximation error}} + \sqrt{\frac{2(n-1)}{N}}, \quad (11)$$

The decomposition leads to the following theoretical insight. Firstly, thanks to the strictly larger working model, SC attains an approximation error that is guaranteed to be no worse than that of LM methods. Secondly, SC estimates $2(n-1)$ parameters—one slope and one intercept per non-reference class—while LM methods estimate only $n-1$ parameters. This leads to a factor of 2 increase in estimation error, which scales with the number of parameters d as $\mathcal{O}(d)$. This gives LM methods an advantage. However, SC incorporates several variance mitigation strategies to actively control estimation error: (i) diverse training instances generated via Algorithm 1; (ii) explicit regularization through the directional trust region constraint and context invariance penalty; and (iii) ensembling procedure in Algorithm 2. These components work in concert to reduce variance and stabilize learning, enabling the model to fully leverage its lower approximation error.

4 Experiments and main results

In this section, we validate the effectiveness of SC by evaluating its classification performance across three LLMs and nine benchmark datasets. SC consistently outperforms all baseline calibration methods across various settings, establishing a new state-of-the-art in ICL for classification.

4.1 Experimental settings

Datasets. We conduct experiments on nine widely used text classification benchmarks spanning sentiment analysis, topic classification, and social media content understanding: SST-2, SST-5 [28], AG News [41], SUBJ [34], TREC [10], Rotten Tomatoes [20], TweetEval-Emotion [18], TweetEval-Hate [1], and Financial PhraseBank [16].

Baselines. We compare SC against 4 label-marginal-based calibration baselines from prior work, namely Base LLM, CC, BC, and DC. Full implementation details and references are provided in Appendix A.

Models. We evaluate SC, CC, DC, and BC on three LLMs: Qwen2-7B-Instruct (Qwen) [38], LLaMA-2-7B-Chat-HF (Llama) [30], and Mistral-7B-Instruct-v0.3 (Mistral) [9]. All models are accessed via the Hugging Face API, and no further fine-tuning is applied.

Other Details. Following prior work, we report Macro-F1 as the primary evaluation metric. Prompts are generated using a fixed template described in Appendix C. We evaluate performance under 4-shot, 8-shot, and 16-shot settings. For each LLM, we run all experiments with 5 random seeds to account for variance due to context sampling. Unless otherwise specified, evaluation is conducted on a held-out test set of 256 examples per dataset.

4.2 Main results

We report the Macro-F1 performance of five calibration methods across 9 datasets, 5 random seeds, and 3 LLMs (Qwen2-7B-Instruct, LLaMA-2-7B-chat-hf, and Mistral-7B-Instruct-v0.3) under 4-, 8-, and 16-shot settings in Figure 3. Specifically, SC consistently achieves the highest Macro-F1 score across all models and shot counts. Compared to the Base LLM, SC yields improvements of up to **+22.6%** absolute in Macro-F1 (8-shot on Qwen2-7B-Instruct), and on average provides **+11.1%** absolute gain across all models and shot configurations. Relative to the strongest competing calibration method (Batch Calibration), SC further improves performance by up to **+13.4%** (16-shot on Mistral-7B-Instruct-v0.3) and achieves an average gain of **+7.1%**. Overall, these results confirm that SC offers a robust and generalizable enhancement of Label-Marginal based calibrations in few-shot learning. In addition, our numerical results are aligned with our theory in presented in Section 3.4. As shown in Figure 3, SC achieves the highest average score among all methods due to better approximation error, but also exhibits increased variance in its performance. More detailed numerical results and comparison are given in Appendix G.

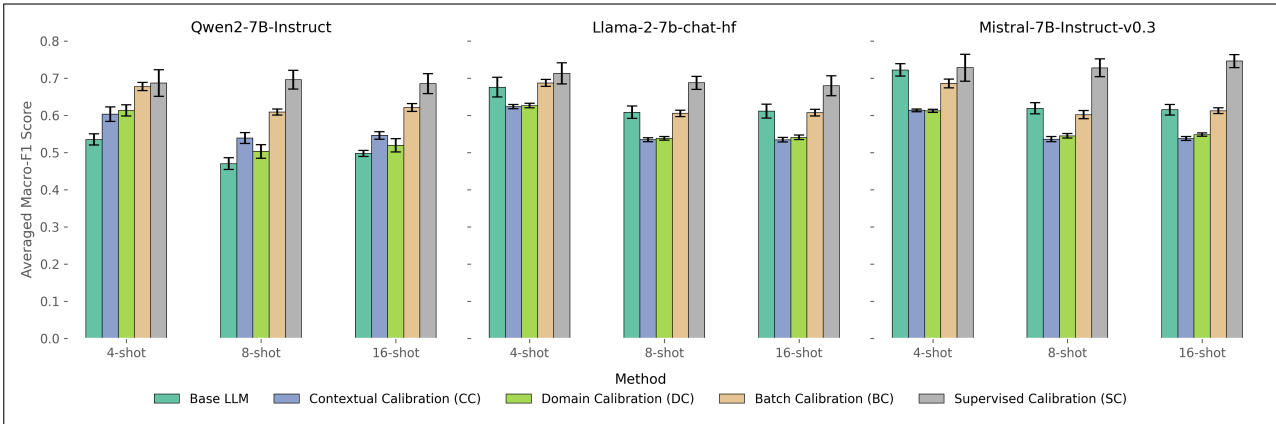


Figure 3: Averaged Macro-F1 scores of five methods across 9 datasets, 3 language models, and 5 random seeds under 4-, 8-, and 16-shot settings. Bars represent the mean performance with standard deviations across datasets.

Furthermore, SC delivers a striking improvement on SST-5: in the 8-shot setting with Qwen, it boosts accuracy from 24% (base LLM) and 25% (other methods) to 44%, nearly doubling performance as shown in Figure 4. This substantial gain stems from SC’s unique ability to not just shift logits, but to reverse the decision boundary when necessary as illustrated in Figure 1. For instance, it learns a bias of -1.29 and a weight of -0.19 for the *negative* class relative to *very negative*. This indicates that SC effectively shifts and reorients the LLM’s decision boundary between closely related classes, enhancing overall performance.

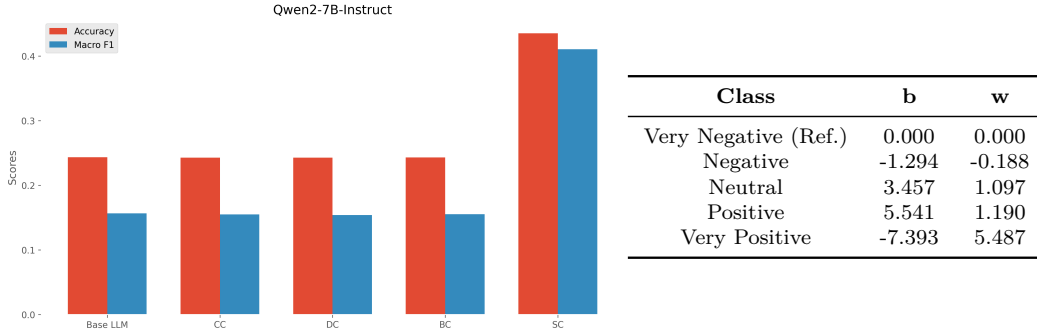


Figure 4: Performance on SST-5 with Qwen2-7B-Instruct in the 8-shot setting, averaged over 5 random seeds. The table on the right shows the average learned coefficients with respect to the *very negative* reference class.

Ablations. We perform ablation studies to understand the contributions of key components within our SC framework. First, we examine the role of the per-class scaling factor. We compare the full SC model with a restricted variant, SC*, in which this factor is fixed to 1—so only the bias term is learned—and include additional baseline calibration methods for reference. In our experiments, SC* outperforms the baselines, indicating that estimating an optimal bias under SC framework is more effective than the methods employed by LM approaches. The full SC model achieves still higher performance than SC*, suggesting that the flexibility to learn the scaling factor—and therefore to both shift and rescale the LLM’s logits—offers a further advantage. Detailed results are provided in Figures 5 and 6 of Appendix H. Second, we assess whether aggregating calibrators trained with different context sizes improves predictive performance. Specifically, we learn a collection of affine-logit models $\{\hat{\theta}^i\}_{i \in I}$, each fitted on training data whose demonstration context contains i examples. Empirically, both accuracy and Macro-F1 increase monotonically as the size of context $|I|$ grows), indicating that calibrators exposed to heterogeneous amounts of contextual information provide complementary signals that improve robustness and overall predictive quality. Detailed results are provided in Figures 7, 8 and 9 of Appendix H.

5 Conclusion

In this paper, we introduce **Supervised Calibration (SC)**, a novel loss-minimization-based calibration framework designed to improve the performance of LLMs in ICL. We design SC to learn a class-specific affine transformation in logit space, allowing it to both shift and reorient the LLM’s decision boundary. Thanks to its expressive functional form, we show that SC generalizes and extends the corrective capabilities of many existing calibration methods for ICL. We further analyze SC through the lens of statistical learning theory, highlighting its approximation-estimation trade-off and providing theoretical insights into

its strengths and limitations relative to prior approaches. Looking ahead, several avenues warrant exploration. Firstly, while our current ensembling strategy averages predictions over randomly selected contexts for each i -shot learner, future work could develop more principled approaches to context selection and weighting, which hold significant potential for improving SC’s performance. Secondly, although we provide theoretical intuition, a more rigorous theoretical analysis of SC, particularly accounting for the statistical dependencies introduced by our surrogate data generation, would be beneficial. Finally, while SC was developed for classification, extending its principles to calibrate LLMs for regression tasks presents an interesting and valuable direction for future research.

References

- [1] V. Basile, C. Bosco, E. Fersini, D. Nozza, V. Patti, F. M. Rangel Pardo, P. Rosso, and M. Sanguinetti. SemEval-2019 task 5: Multilingual detection of hate speech against immigrants and women in Twitter. In J. May, E. Shutova, A. Herbelot, X. Zhu, M. Apidianaki, and S. M. Mohammad, editors, *Proceedings of the 13th International Workshop on Semantic Evaluation*, pages 54–63, Minneapolis, Minnesota, USA, June 2019. Association for Computational Linguistics. doi: 10.18653/v1/S19-2007. URL <https://aclanthology.org/S19-2007/>.
- [2] T. B. Brown, B. Mann, N. Ryder, and et al. Language models are few-shot learners. In *Advances in Neural Information Processing Systems (NeurIPS)*, 2020.
- [3] H. Cho, Y. Sakai, M. Kato, K. Tanaka, A. Ishii, and N. Inoue. Token-based decision criteria are suboptimal in in-context learning. *arXiv preprint arXiv:2406.16535*, 2024.
- [4] Y. Cui, H. Lu, and S. Joty. Decoder tuning: Lightweight adaptation for robust in-context learning. *arXiv preprint arXiv:2310.12345*, 2023.
- [5] Y. Fei, Y. Hou, Z. Chen, and A. Bosselut. Mitigating label biases for in-context learning. In *Proceedings of ACL*, pages 14014–14031, 2023.
- [6] Z. Han, Y. Hao, L. Dong, Y. Sun, and F. Wei. Prototypical calibration for few-shot learning of language models. *arXiv preprint arXiv:2205.10183*, 2022.
- [7] A. Holtzman, P. West, Y. Choi, and et al. Surface form competition: Why the highest probability answer isn’t always right. In *Empirical Methods in Natural Language Processing (EMNLP)*, 2021.
- [8] A. Holtzman, P. West, V. Shwartz, Y. Choi, and L. Zettlemoyer. Surface form competition: Why the highest probability answer isn’t always right. *arXiv preprint arXiv:2104.08315*, 2021.

- [9] A. Q. Jiang, A. Sablayrolles, A. Mensch, C. Bamford, D. S. Chaplot, D. de las Casas, F. Bressand, G. Lengyel, G. Lample, L. Saulnier, L. R. Lavaud, M.-A. Lachaux, P. Stock, T. L. Scao, T. Lavril, T. Wang, T. Lacroix, and W. E. Sayed. Mistral 7b, 2023. URL <https://arxiv.org/abs/2310.06825>.
- [10] X. Li and D. Roth. Learning question classifiers. In *COLING 2002: The 19th International Conference on Computational Linguistics*, 2002. URL <https://aclanthology.org/C02-1150/>.
- [11] Liangchen Xu, Xiaoxin Zhang, and Diyi Yang. knn-icl: Nearest-neighbour label assignment for few-shot inference. In *Proc. ACL*, 2023.
- [12] J. Liu, C. Zheng, P. Fung, and et al. Multi-demonstration aggregation for robust in-context learning. In *Association for Computational Linguistics (ACL)*, 2022.
- [13] P. Liu and et al. Evaluating the in-context learning ability of foundation models. *arXiv preprint*, 2023.
- [14] Y. Liu, S. Feng, and C. Tan. Active example selection for in-context learning. In *Proc. EMNLP*, 2022.
- [15] X. Lu, D. Narayanan, M. Zaharia, and J. Zou. What makes a good order of examples in in-context learning? In *Proc. EMNLP Findings*, 2022.
- [16] P. Malo, A. Sinha, P. Korhonen, J. Wallenius, and P. Takala. Good debt or bad debt: Detecting semantic orientations in economic texts. *Journal of the Association for Information Science and Technology*, 65(4):782–796, 2014.
- [17] S. Min, M. Lewis, and H. Hajishirzi. Rethinking the role of demonstrations: What makes in-context learning work? In *Transactions of the Association for Computational Linguistics (TACL)*, 2022.
- [18] S. Mohammad, F. Bravo-Marquez, M. Salameh, and S. Kiritchenko. SemEval-2018 task 1: Affect in tweets. In M. Apidianaki, S. M. Mohammad, J. May, E. Shutova, S. Bethard, and M. Carpuat, editors, *Proceedings of the 12th International Workshop on Semantic Evaluation*, pages 1–17, New Orleans, Louisiana, June 2018. Association for Computational Linguistics. doi: 10.18653/v1/S18-1001. URL <https://aclanthology.org/S18-1001/>.
- [19] X. Pan, Y. Wang, X. Liu, and et al. Coverage-based example selection for in-context learning. In *Proc. EMNLP Findings*, 2023.
- [20] B. Pang and L. Lee. Seeing stars: Exploiting class relationships for sentiment categorization with respect to rating scales. *arXiv preprint cs/0506075*, 2005.

- [21] P. Pezeshkpour and E. Hruschka. Large language models sensitivity to the order of options in multiple-choice questions. *arXiv preprint arXiv:2308.11483*, 2023.
- [22] Y. Razeghi, E. Perez, D. Kiela, and Y. Tay. Impact of pre-training term frequencies on few-shot reasoning. In *Proc. ACL*, 2022.
- [23] B. Rubin, J. Herzig, and J. Berant. Learning to retrieve demonstrations for in-context learning. In *Proc. EMNLP*, 2022.
- [24] J. Schulman, S. Levine, P. Abbeel, M. Jordan, and P. Moritz. Trust region policy optimization. In *International conference on machine learning*, pages 1889–1897. PMLR, 2015.
- [25] Seongjoo Min, Ximing Liu, and Mohit Iyyer. Noisy channel prompting for robust in-context learning. In *Proc. ACL*, 2022.
- [26] S. Shin, S. Lee, H. Ahn, and et al. On the effect of pre-training corpora on in-context learning. In *Proc. ACL*, 2022.
- [27] C. Si, D. Friedman, N. Joshi, S. Feng, D. Chen, and H. He. Measuring inductive biases of in-context learning with underspecified demonstrations. In *Proceedings of ACL*, pages 11289–11310, 2023.
- [28] R. Socher, A. Perelygin, J. Wu, J. Chuang, C. D. Manning, A. Ng, and C. Potts. Recursive deep models for semantic compositionality over a sentiment treebank. In D. Yarowsky, T. Baldwin, A. Korhonen, K. Livescu, and S. Bethard, editors, *Proceedings of the 2013 Conference on Empirical Methods in Natural Language Processing*, pages 1631–1642, Seattle, Washington, USA, Oct. 2013. Association for Computational Linguistics. URL <https://aclanthology.org/D13-1170/>.
- [29] J. Sørensen and A. Søgaard. Template selection via mutual information for in-context learning. In *Proc. EMNLP*, 2022.
- [30] H. Touvron, L. Martin, K. Stone, P. Albert, A. Almahairi, Y. Babaei, N. Bashlykov, S. Batra, P. Bhargava, S. Bhosale, D. Bikel, L. Blecher, C. C. Ferrer, M. Chen, G. Cucurull, D. Esiobu, J. Fernandes, J. Fu, W. Fu, B. Fuller, C. Gao, V. Goswami, N. Goyal, A. Hartshorn, S. Hosseini, R. Hou, H. Inan, M. Kardas, V. Kerkez, M. Khabsa, I. Kloumann, A. Korenev, P. S. Koura, M.-A. Lachaux, T. Lavril, J. Lee, D. Liskovich, Y. Lu, Y. Mao, X. Martinet, T. Mihaylov, P. Mishra, I. Molybog, Y. Nie, A. Poulton, J. Reizenstein, R. Rungta, K. Saladi, A. Schelten, R. Silva, E. M. Smith, R. Subramanian, X. E. Tan, B. Tang, R. Taylor, A. Williams, J. X. Kuan, P. Xu, Z. Yan, I. Zarov, Y. Zhang, A. Fan, M. Kambadur, S. Narang, A. Rodriguez, R. Stojnic, S. Edunov, and T. Scialom. Llama 2: Open foundation and fine-tuned chat models, 2023. URL <https://arxiv.org/abs/2307.09288>.

- [31] X. Wan and colleagues. Confidence-guided example selection for in-context learning. *arXiv preprint arXiv:2309.17249*, 2023.
- [32] X. Wan, R. Sun, H. Dai, and et al. Consistency-based self-adaptive prompting. *arXiv preprint arXiv:2305.14106*, 2023.
- [33] P. Wang, L. Li, L. Chen, D. Zhu, and *et al.* Large language models are not fair evaluators. *arXiv preprint arXiv:2305.17926*, 2023.
- [34] S. I. Wang and C. D. Manning. Baselines and bigrams: Simple, good sentiment and topic classification. In *Proceedings of the 50th Annual Meeting of the Association for Computational Linguistics (Volume 2: Short Papers)*, pages 90–94, 2012.
- [35] J. Wei, J. Wei, Y. Tay, and et al. Larger language models can learn new input–label mappings in context. *arXiv preprint arXiv:2303.03846*, 2023.
- [36] T. Wolf, L. Debut, V. Sanh, J. Chaumond, C. Delangue, A. Moi, P. Cistac, T. Rault, R. Louf, M. Funtowicz, et al. Transformers: State-of-the-art natural language processing. In *Proceedings of the 2020 conference on empirical methods in natural language processing: system demonstrations*, pages 38–45, 2020.
- [37] S. Xie, A. Raghunathan, P. Liang, and Tengyu Ma. An explanation of in-context learning as implicit bayesian inference. In *Proc. ICLR*, 2022.
- [38] A. Yang, B. Yang, B. Hui, B. Zheng, B. Yu, C. Zhou, C. Li, C. Li, D. Liu, F. Huang, G. Dong, H. Wei, H. Lin, J. Tang, J. Wang, J. Yang, J. Tu, J. Zhang, J. Ma, J. Yang, J. Xu, J. Zhou, J. Bai, J. He, J. Lin, K. Dang, K. Lu, K. Chen, K. Yang, M. Li, M. Xue, N. Ni, P. Zhang, P. Wang, R. Peng, R. Men, R. Gao, R. Lin, S. Wang, S. Bai, S. Tan, T. Zhu, T. Li, T. Liu, W. Ge, X. Deng, X. Zhou, X. Ren, X. Zhang, X. Wei, X. Ren, X. Liu, Y. Fan, Y. Yao, Y. Zhang, Y. Wan, Y. Chu, Y. Liu, Z. Cui, Z. Zhang, Z. Guo, and Z. Fan. Qwen2 technical report, 2024. URL <https://arxiv.org/abs/2407.10671>.
- [39] J. Ye, M. Ding, P. Liu, and J. Fu. Flipped learning mitigates label noise in in-context learning. In *Proc. NAACL*, 2023.
- [40] Y. Yin, M. Fang, and T. Cohn. Template optimization for robust in-context learning. In *Proc. ACL*, 2023.
- [41] X. Zhang, J. Zhao, and Y. LeCun. Character-level convolutional networks for text classification. *Advances in neural information processing systems*, 28, 2015.
- [42] Z. Zhao, E. Wallace, S. Feng, D. Klein, and S. Singh. Calibrate before use: Improving few-shot performance of language models. In *International conference on machine learning*, pages 12697–12706. PMLR, 2021.

- [43] W. Zheng and colleagues. Pride: Permutation debiasing for multiple-choice evaluation with large language models. *arXiv preprint arXiv:2307.XXXXX*, 2023.
- [44] H. Zhou, X. Wan, L. Proleev, D. Mincu, J. Chen, K. Heller, and S. Roy. Batch calibration: Rethinking calibration for in-context learning and prompt engineering. *arXiv preprint arXiv:2309.17249*, 2023.

A Implementation details

Computation Resources. All large language models (LLMs) used in our experiments are based on publicly available implementations from the **Hugging Face Transformers** library [36]. We conduct all experiments on a dedicated computing node equipped with 8 NVIDIA A6000 Ada Generation GPUs.

Contextual Calibration [42](CC) Following the original CC implementation, we compute the label probabilities conditioned on each of the three content-free tokens—‘N/A’, ‘,’ and ‘[MASK]’—along with the context. We then take the mean of these probabilities and use it to normalize the LLM’s label-space probabilities computed for the test query and the same context.

Domain-Context Calibration [5] We reproduce the DC baseline by using the test set as the unlabeled corpus to construct a bag-of-words. From this bag, we randomly sample tokens to create content-free and in-domain inputs with an average target length. Following [5], this process is repeated 20 times, and we compute the mean probability over these samples. Following the original implementation, we use this mean to normalize the LLM’s label-space probabilities computed for the test query and context.

Batch Calibration [44] (BC) BC is an inference-time calibration method that computes the mean of label probabilities over m test samples given the context during the inference. We set $m = 128$ and use this mean to normalize the LLM’s label-space probabilities given the test query and context.

Supervised Calibration (SC) We adopt an ensembling strategy for SC as outlined in Algorithm 2. For each configuration— $k = 4$, $k = 8$, and $k = 16$ —we set the minimum context size i_{\min} (as defined in Algorithm 2) to 1, and the maximum context size i_{\max} to $\min(5, k - 1)$. We fix the regularization parameter λ_{inv} to 10 across all settings and LLMs. Additionally, the number of context to be sampled from $\mathcal{C}(i)$ (given in Definition 1) for size i during the inference is set as:

$$m_i = \min \left(\left\lfloor \frac{|\mathcal{T}_i|}{2} \right\rfloor, 24 \right),$$

where $|\mathcal{T}_i|$ denotes the number of available samples for context size i outputted by Algorithm 1.

To determine the value of τ , we use the following formulation:

$$\tau = \arccos(\theta)$$

We first compute the in-sample accuracy of the LLM while generating the training data through Algorithm 1. Based on this accuracy, we set the value of θ as follows:

$$\theta = \begin{cases} (20^\circ)^{\frac{1}{K-1}} & \text{if accuracy} \geq 0.9 \\ (45^\circ)^{\frac{1}{K-1}} & \text{if } 0.7 \leq \text{accuracy} < 0.9 \\ (90^\circ)^{\frac{1}{K-1}} & \text{if } 0.5 \leq \text{accuracy} < 0.7 \\ 180^\circ & \text{if accuracy} < 0.5 \end{cases}$$

Here, K denotes the number of distinct labels in the dataset.

While running SC with the setting $k = 4$, we excluded datasets containing more than four classes (i.e SST5 and TREC). This is because when the number of classes exceeds the number of context examples, some classes are inevitably left out of the training data. This imbalance poses a challenge for training logistic regression models across different context sizes.

B Additional related work

Mechanisms and prompt Optimization for ICL Another line of work diagnoses why LLMs succeed or fail at ICL. The performance of a fixed prompt can swing from near random-guess to state of the art when the order of demonstrations is permuted [15], and it correlates strongly with the pre-training statistics of the tokens that appear in the prompt [22, 26]. From a theoretical perspective, ICL has been interpreted as implicit Bayesian inference in sequence models [37], while empirical evidence shows that sufficiently large models can even override entrenched semantic priors to learn arbitrary input-label mappings on the fly [35]. A complementary literature focuses on controlling these factors. Template-search methods [29, 19, 40] and example-selection algorithms [23, 14, 32] systematically pick demonstrations that maximize mutual information or diversity, while Wan and colleagues [31] add consistency and repetition checks. To make ICL more robust, researchers have proposed noisy-channel prompting [25], flipped learning that trains the model against label noise [39], k-nearest-neighbour label assignment [11], and lightweight decoder networks that adapt the prompt at inference time [4]. Together, these studies paint a converging picture: effective ICL hinges on matching the prompt (template *and* examples) to the model’s pre-training biases—then compensating for the remaining mismatches with task-specific selection or robust inference techniques.

C Prompt templates

Table 1: Prompt templates and label words for various datasets.

| Dataset | Prompt Template | Label Words |
|--------------|-------------------------------|---|
| SST2 | sentence: <x>\nsentiment: <y> | negative, positive |
| SST5 | sentence: <x>\nsentiment: <y> | terrible, bad, neutral, good, great |
| Rotten T. | review: <x>\nsentiment: <y> | negative, positive |
| Financial P. | sentence: <x>\nsentiment: <y> | negative, neutral, positive |
| Subj | review: <x>\ntype: <y> | objective, subjective |
| TREC | question: <x>\ntarget: <y> | abbreviation, entity, description, person, location, number |
| AGNews | news: <x>\ntopic: <y> | world, sports, business, technology |
| TE-Emo | tweet: <x>\nemotion: <y> | anger, joy, optimism, sadness |
| TE-Hate | tweet: <x>\nhate speech: <y> | non-hate, hate |

D Additional notation and detailed formulation

Let $C_k = \{e^{(1)}, e^{(2)}, \dots, e^{(k)}\}$ be the full demonstration set of k unique input-label exemplars, where $e^{(l)} = (x^{(l)}, y^{(l)})$.

Definition 1 (Set of Ordered Contexts) *The set $\mathcal{C}(i)$ is defined as:*

$$\mathcal{C}(i) = \{(s_1, s_2, \dots, s_i) \mid s_j \in C_k \text{ for } j = 1, \dots, i; \text{ and } s_j \neq s_p \text{ for } j \neq p\}. \quad (12)$$

This set comprises all distinct ordered sequences (permutations) of i unique exemplars chosen from the full demonstration set C_k .

Definition 2 (Set of Contexts Used for Query x) *Given an exemplar $(x, y) \in C_k$, let \mathcal{T}_i be the surrogate training dataset generated by Algorithm 1 using contexts of size i from C_k . The set $\mathcal{C}(x, i)$ is defined as:*

$$\mathcal{C}(x, i) = \{C_i^{(j)} \in \mathcal{C}(i) \mid (x, y) \notin C_i^{(j)} \text{ and } (m(x; C_i^{(j)}), y) \in \mathcal{T}_i\}. \quad (13)$$

This set consists of all ordered contexts of size i from $\mathcal{C}(i)$ that do not contain the specific exemplar (x, y) itself, and were actually used to generate a (logit, label) pair for the query x within the surrogate training data \mathcal{T}_i .

Definition 3 (Context Invariance Regularization Penalty) *The total Context Invariance Regularization Penalty for parameters θ^i is defined as:*

$$\text{InvPenalty}(\theta^i) = \sum_{x \in \{x_l \mid (x^{(l)}, y^{(l)}) \in C_k\}} \sum_{\{C_i^{(a)}, C_i^{(b)}\} \subseteq \mathcal{C}(x, i), a \neq b} L_{\text{sym}}(\theta^i, x, C_i^{(a)}, C_i^{(b)}). \quad (14)$$

This penalty aggregates the symmetric cross-entropy loss over all distinct pairs of contexts $(C_i^{(a)}, C_i^{(b)})$ that were used to evaluate each unique query input x derived from the original demonstration set C_k . It encourages the calibrated predictions for the same query x to be consistent, regardless of the specific context $C_i^{(j)} \in \mathcal{C}(x, i)$ used to generate the intermediate LLM logits.

Table 2: Summary of Label Marginal based calibration methods. Each method adjusts the LLM prediction $P_{\text{LLM}}(y | x, C_k)$ via the different estimators of $P_{\text{LLM}}(y|C_k)$.

| Method | Formula | Description |
|---------------------------------|---|---|
| Base LLM | $\arg \max_y P_{\text{LLM}}(y x, C_k)$ | Select the label with the highest conditional probability from the LLM. |
| Contextual Calibration (CC) | $\arg \max_y \frac{P_{\text{LLM}}(y x, C_k)}{P_{\text{LLM}}(y \text{NA}, C_k)}$ | Normalize the prediction using a content-free input. |
| Domain-Context Calibration (DC) | $\arg \max_y \frac{P_{\text{LLM}}(y x, C_k)}{\frac{1}{N} \sum_i P_{\text{LLM}}(y \text{RandDom}_i, C_k)}$ | Use randomly sampled domain prompts as a reference for normalization. |
| Batch Calibration (BC) | $\arg \max_y \frac{P_{\text{LLM}}(y x, C_k)}{\frac{1}{N} \sum_i P_{\text{LLM}}(y x_i, C_k)}$ | Calibrate by averaging predictions over a batch of reference inputs. |

E Surrogate data generation algorithm

Algorithm 1 Surrogate Data Generation for Calibration

Require: Demonstration set $C_k = \{(x^{(l)}, y^{(l)})\}_{l=1}^k$ of size k .

Require: Target context size i such that $1 \leq i < k$.

Require: LM inference function $\text{Infer}(x, C_i)$ that returns logit vector $\mathbf{m}(x; C_i)$.

- 1: Initialize training set $\mathcal{T}_i \leftarrow \emptyset$.
 - 2: Generate $\mathcal{C}(i)$, the set of all distinct ordered subsets of C_k with size i . ▷ E.g., permutations of C_k , taking first i .
 - 3: **for** each context $C_i^{(a)} \in \mathcal{C}(i)$ **do**
 - 4: Define the held-out set $R_i^{(a)} \leftarrow C_k \setminus C_i^{(a)}$. ▷ Set difference based on elements.
 - 5: **for** each query (x, y) in $R_i^{(a)}$ **do**
 - 6: Compute model logits vector: $\mathbf{m}(x; C_i^{(a)}) \leftarrow \text{Infer}(x, C_i^{(a)})$.
 - 7: Add to training set: $\mathcal{T}_i \leftarrow \mathcal{T}_i \cup \{(\mathbf{m}(x; C_i^{(a)}), y)\}$. ▷ Store feature vector and true label.
 - 8: **end for**
 - 9: **end for**
 - 10: **Output:** Training set \mathcal{T}_i consisting of pairs (model logits, true label).
-

F Full algorithm

Algorithm 2 SC (Full Procedure)

Require: Full demonstration set $C_k = \{(x^{(l)}, y^{(l)})\}_{l=1}^k$; Set of context sizes $I = \{i_{min}, \dots, i_{max}\}$; Regularization $\lambda_{inv} \geq 0$, $\tau \in [0, 1]$; Context samples $m_i \geq 1$; Query x ; Inference function $\text{Infer}(x, C)$ returns logit vector $\mathbf{m}(x, C)$.

Part 1: Training Phase

- 1: Initialize parameter set $\Theta \leftarrow \emptyset$.
- 2: **for** each context size $i \in I$ **do**
- 3: Generate training data \mathcal{T}_i using Algorithm 1 with C_k .
- 4: Learn parameters $\hat{\theta}^i$ by solving Eq. (8) using \mathcal{T}_i , λ_{inv} , τ .
- 5: Store $\hat{\theta}^i$ in Θ .
- 6: **end for**

Part 2: Prediction Phase (for query x)

- 7: Initialize list $P_{\text{list}} \leftarrow []$.
 - 8: **for** each context size $i \in I$ **do**
 - 9: Sample index set $\mathcal{M}_i \subseteq \{1, \dots, |\mathcal{C}(i)|\}$ uniformly at random such that $|\mathcal{M}_i| = m_i$.
 - 10: Retrieve learned parameters $\hat{\theta}^i$ from Θ .
 - 11: Retrieve sub-contexts $\{C_i^{(j)}\}_{j \in \mathcal{M}_i}$ from $\mathcal{C}(i)$ using \mathcal{M}_i .
 - 12: Initialize list $p_{\text{list}}^{(i)} \leftarrow []$.
 - 13: **for** $j \in \mathcal{M}_i$ **do**
 - 14: $\mathbf{m}(x, C_i^{(j)}) \leftarrow \text{Infer}(x, C_i^{(j)})$.
 - 15: $\mathbf{p}^{(j)}(x) \leftarrow \mathbf{f}(m(x, C_i^{(j)}); \hat{\theta}^i)$.
 - 16: Append $\mathbf{p}^{(j)}(x)$ to $p_{\text{list}}^{(i)}$.
 - 17: **end for**
 - 18: $\hat{\mathbf{p}}_i(x) \leftarrow \frac{1}{m_i} \sum_{\mathbf{p}(x) \in p_{\text{list}}^{(i)}} \mathbf{p}(x)$.
 - 19: Append $\hat{\mathbf{p}}_i(x)$ to P_{list} .
 - 20: **end for**
 - 21: $\hat{\mathbf{p}}_{\text{SC}}(x) \leftarrow \frac{1}{|I|} \sum_{\mathbf{p}(x) \in P_{\text{list}}} \mathbf{p}(x)$.
 - 22: **Output:** $\hat{y}_{\text{SC}} \in \arg \max_{y_c \in \mathcal{Y}} [\hat{\mathbf{p}}_{\text{SC}}(x)]_c$.
-

G Detailed numerical results

In this section, we present detailed numerical results. For brevity, we refer to Qwen2-7B-Instruct, Llama-2-7b-chat-hf, and Mistral-7B-Instruct-v0.3 as Qwen, Llama, and Mistral, respectively, throughout the remainder of this section.

Table 3: Average Macro-F1 scores (%) for various calibration methods on selected datasets, evaluated for each LLM in the 4-shot setting ($k = 4$) over five random seeds. Values are presented as mean_{standard deviation}, with the highest score in each column highlighted in **bold** and shaded gray.

| Model | Method | Avg | AGNews | FPB | SST2 | RT | Subj | TE-Emo | TE-Hate |
|---------|----------|--------------|------------------------------|------------------------------|------------------------------|------------------------------|-------------------------------|------------------------------|------------------------------|
| Qwen | Base LLM | 53.49 | 62.74 _{1.56} | 31.22 _{9.82} | 87.74 _{7.42} | 88.23 _{1.90} | 33.02 _{0.81} | 35.23 _{1.53} | 36.26 _{0.20} |
| | CC | 60.30 | 85.22 _{4.97} | 51.46 _{10.52} | 91.63 _{0.78} | 89.91 _{1.35} | 38.54 _{7.64} | 35.07 _{5.54} | 30.25 _{0.00} |
| | DC | 61.30 | 88.68 _{0.68} | 52.86 _{10.45} | 87.20 _{5.76} | 90.31 _{0.90} | 36.97 _{3.72} | 42.82 _{2.33} | 30.25 _{0.00} |
| | BC | 67.71 | 70.14 _{2.17} | 73.54 _{2.75} | 88.92 _{5.77} | 90.18 _{1.41} | 74.10 _{3.92} | 40.94 _{3.24} | 36.16 _{0.00} |
| | SC | 68.66 | 72.76 _{6.13} | 75.57 _{6.67} | 90.11 _{4.99} | 89.39 _{1.76} | 62.23 _{11.15} | 41.25 _{17.51} | 49.33 _{8.08} |
| Llama | Base LLM | 67.57 | 77.58 _{7.17} | 66.41 _{5.92} | 93.36 _{0.44} | 91.16 _{1.59} | 40.18 _{12.93} | 67.34 _{6.12} | 36.94 _{7.64} |
| | CC | 62.31 | 71.01 _{3.42} | 81.86 _{2.72} | 93.17 _{1.02} | 92.07 _{0.96} | 32.36 _{0.00} | 35.45 _{0.76} | 30.25 _{0.00} |
| | DC | 62.61 | 72.10 _{3.61} | 82.94 _{2.82} | 93.60 _{0.50} | 91.95 _{1.18} | 32.36 _{0.00} | 35.06 _{1.02} | 30.25 _{0.00} |
| | BC | 68.69 | 66.06 _{2.04} | 84.56 _{3.75} | 93.53 _{0.47} | 91.52 _{1.28} | 54.15 _{3.48} | 36.29 _{1.38} | 51.70 _{2.00} |
| | SC | 71.28 | 71.76 _{11.31} | 84.02 _{4.70} | 94.25 _{0.53} | 91.56 _{1.19} | 55.79 _{11.41} | 55.35 _{10.57} | 46.20 _{4.31} |
| Mistral | Base LLM | 72.20 | 79.28 _{6.90} | 89.55 _{1.92} | 94.07 _{0.75} | 92.47 _{0.62} | 35.03 _{6.42} | 60.53 _{9.67} | 54.51 _{9.67} |
| | CC | 61.34 | 63.47 _{1.91} | 87.24 _{1.10} | 94.76 _{0.70} | 92.39 _{0.75} | 31.55 _{0.00} | 32.11 _{1.24} | 27.89 _{0.00} |
| | DC | 61.17 | 63.29 _{1.29} | 86.08 _{2.53} | 94.17 _{0.20} | 92.39 _{0.75} | 31.55 _{0.00} | 32.82 _{1.37} | 27.89 _{0.00} |
| | BC | 68.57 | 62.81 _{1.11} | 86.66 _{2.32} | 94.00 _{0.69} | 92.63 _{0.67} | 48.05 _{6.53} | 34.08 _{2.67} | 61.73 _{2.67} |
| | SC | 72.78 | 75.66 _{11.50} | 90.93 _{2.52} | 95.07 _{1.15} | 91.53 _{2.51} | 59.38 _{12.89} | 59.48 _{9.90} | 37.40 _{16.36} |

Table 4: Average Macro-F1 scores (%) for various calibration methods on selected datasets, evaluated for each LLM in the 8-shot setting ($k = 8$) over five random seeds. Values are presented as mean_{standard deviation}, with the highest score in each column highlighted in **bold** and shaded gray.

| Model | Method | Avg | SST5 | TREC | AGNews | FPB | SST2 | RT | Subj | TE-Emo | TE-Hate |
|---------|----------|--------------|------------------------------|------------------------------|------------------------------|------------------------------|------------------------------|------------------------------|------------------------------|-------------------------------|-------------------------------|
| Qwen | Base LLM | 47.00 | 15.65 _{0.33} | 45.40 _{5.99} | 62.06 _{0.79} | 30.13 _{2.09} | 74.65 _{18.64} | 91.00 _{2.28} | 31.55 _{0.00} | 34.55 _{2.41} | 38.01 _{0.00} |
| | CC | 53.91 | 15.48 _{0.14} | 63.30 _{5.09} | 82.27 _{6.74} | 35.96 _{7.09} | 89.00 _{2.59} | 92.30 _{1.37} | 32.67 _{0.96} | 46.29 _{5.54} | 27.89 _{0.00} |
| | DC | 50.26 | 15.41 _{0.07} | 43.83 _{3.18} | 86.86 _{0.90} | 35.92 _{3.97} | 69.94 _{19.04} | 91.09 _{1.48} | 34.69 _{4.03} | 46.74 _{3.82} | 27.89 _{0.00} |
| | BC | 60.88 | 15.52 _{0.12} | 67.98 _{1.73} | 65.36 _{1.18} | 66.87 _{2.90} | 86.43 _{4.45} | 91.95 _{1.40} | 76.89 _{1.32} | 38.88 _{3.00} | 38.01 _{0.00} |
| | SC | 69.59 | 41.06 _{2.80} | 61.28 _{4.30} | 85.32 _{4.37} | 74.97 _{6.19} | 91.36 _{3.75} | 90.64 _{2.56} | 70.94 _{4.35} | 57.09 _{19.29} | 53.63 _{3.26} |
| Llama | Base LLM | 60.82 | 15.75 _{1.31} | 44.60 _{4.29} | 74.55 _{4.43} | 80.26 _{2.73} | 94.15 _{1.11} | 91.94 _{1.17} | 37.54 _{5.96} | 68.74 _{3.60} | 39.86 _{8.28} |
| | CC | 53.44 | 30.61 _{1.13} | 24.68 _{2.68} | 64.66 _{1.50} | 80.97 _{2.81} | 94.59 _{0.75} | 92.40 _{0.72} | 31.55 _{0.00} | 33.64 _{1.28} | 27.89 _{0.00} |
| | DC | 53.80 | 30.91 _{1.25} | 25.52 _{3.12} | 65.73 _{0.68} | 82.44 _{1.86} | 94.47 _{1.29} | 92.47 _{0.62} | 31.55 _{0.00} | 33.25 _{1.10} | 27.89 _{0.00} |
| | BC | 60.52 | 23.49 _{0.80} | 36.22 _{1.47} | 63.78 _{1.27} | 82.71 _{3.05} | 94.09 _{1.38} | 92.01 _{1.03} | 65.21 _{4.20} | 33.56 _{1.15} | 53.59 _{2.51} |
| | SC | 68.74 | 42.76 _{4.23} | 39.78 _{10.65} | 86.01 _{2.85} | 85.58 _{2.04} | 95.27 _{0.51} | 92.53 _{1.24} | 61.89 _{4.20} | 66.78 _{5.65} | 48.05 _{3.83} |
| Mistral | Base LLM | 61.86 | 14.66 _{0.25} | 40.08 _{5.39} | 70.59 _{3.84} | 85.80 _{4.22} | 94.41 _{1.75} | 92.61 _{0.45} | 37.20 _{4.35} | 61.82 _{3.01} | 59.55 _{6.75} |
| | CC | 53.70 | 28.22 _{1.26} | 27.80 _{3.47} | 62.29 _{1.42} | 84.64 _{4.39} | 94.23 _{1.79} | 92.69 _{0.40} | 31.55 _{0.00} | 32.95 _{1.02} | 27.89 _{0.00} |
| | DC | 54.47 | 31.15 _{1.38} | 30.17 _{3.26} | 62.07 _{0.58} | 83.59 _{3.07} | 94.68 _{1.56} | 92.70 _{0.46} | 31.55 _{0.00} | 33.43 _{0.80} | 27.89 _{0.00} |
| | BC | 60.16 | 24.83 _{0.54} | 40.26 _{4.25} | 61.58 _{0.97} | 83.59 _{3.07} | 94.19 _{1.52} | 92.62 _{0.67} | 48.26 _{7.71} | 32.91 _{1.05} | 63.25 _{2.06} |
| | SC | 72.77 | 45.44 _{3.01} | 48.57 _{8.36} | 86.84 _{3.42} | 88.54 _{4.70} | 93.24 _{1.58} | 90.09 _{1.73} | 66.91 _{6.13} | 67.73 _{7.99} | 67.53 _{11.74} |

Table 5: Average Macro-F1 scores (%) for various calibration methods on selected datasets, evaluated for each LLM in the 16-shot setting ($k = 16$) over five random seeds. Values are presented as mean_{standard deviation}, with the highest score in each column highlighted in **bold** and shaded gray.

| Model | Method | Avg | SST5 | TREC | AGNews | FPB | SST2 | RT | Subj | TE-Emo | TE-Hate |
|---------|----------|--------------|------------------------------|------------------------------|------------------------------|------------------------------|------------------------------|------------------------------|-------------------------------|------------------------------|-------------------------------|
| Qwen | Base LLM | 49.75 | 14.47 _{0.29} | 59.68 _{5.52} | 63.10 _{0.85} | 26.72 _{0.84} | 87.55 _{6.49} | 91.56 _{1.80} | 31.55 _{0.00} | 35.15 _{0.56} | 38.01 _{0.00} |
| | CC | 54.57 | 14.41 _{0.21} | 69.40 _{1.31} | 85.30 _{2.77} | 27.16 _{9.25} | 92.40 _{0.89} | 93.32 _{0.66} | 37.69 _{4.80} | 43.58 _{0.71} | 27.89 _{0.00} |
| | DC | 51.92 | 14.38 _{0.21} | 44.43 _{3.81} | 88.07 _{0.78} | 39.48 _{14.78} | 83.91 _{9.82} | 93.42 _{1.05} | 35.32 _{4.41} | 40.41 _{1.50} | 27.89 _{0.00} |
| | BC | 62.12 | 14.64 _{0.36} | 72.75 _{3.37} | 69.02 _{3.35} | 68.42 _{8.43} | 91.30 _{0.91} | 92.64 _{0.89} | 76.63 _{3.03} | 35.63 _{0.92} | 38.01 _{0.00} |
| | SC | 68.52 | 39.32 _{6.66} | 69.91 _{2.56} | 85.34 _{3.34} | 66.57 _{9.62} | 92.95 _{2.10} | 92.15 _{1.39} | 66.03 _{10.62} | 53.63 _{6.91} | 50.76 _{10.97} |
| Llama | Base LLM | 60.72 | 14.49 _{0.64} | 54.93 _{5.18} | 75.64 _{5.72} | 76.74 _{5.43} | 94.25 _{0.65} | 92.01 _{1.17} | 37.00 _{4.14} | 69.33 _{9.55} | 35.71 _{2.64} |
| | CC | 53.42 | 31.40 _{1.16} | 24.02 _{4.02} | 63.73 _{1.29} | 81.60 _{2.58} | 94.41 _{1.19} | 92.78 _{0.67} | 31.55 _{0.00} | 33.37 _{1.09} | 27.89 _{0.00} |
| | DC | 54.06 | 32.09 _{1.25} | 25.52 _{3.12} | 65.54 _{0.68} | 83.80 _{3.50} | 94.59 _{1.19} | 92.47 _{0.62} | 31.55 _{0.00} | 32.35 _{1.10} | 27.89 _{0.00} |
| | BC | 60.72 | 24.61 _{1.12} | 32.62 _{3.83} | 63.85 _{0.57} | 83.37 _{3.68} | 94.46 _{0.85} | 92.46 _{1.03} | 65.81 _{2.42} | 33.64 _{1.28} | 56.26 _{4.20} |
| | SC | 67.95 | 42.76 _{4.23} | 62.21 _{5.62} | 87.09 _{2.82} | 79.81 _{8.37} | 93.81 _{0.71} | 91.83 _{1.46} | 50.65 _{15.60} | 62.21 _{4.15} | 46.72 _{10.59} |
| Mistral | Base LLM | 61.49 | 14.42 _{0.15} | 45.48 _{4.45} | 71.17 _{2.31} | 84.17 _{3.03} | 93.87 _{0.79} | 92.39 _{0.73} | 37.69 _{3.27} | 70.79 _{4.21} | 43.42 _{9.60} |
| | CC | 53.75 | 28.96 _{1.12} | 28.97 _{3.71} | 63.38 _{0.91} | 82.73 _{2.58} | 93.93 _{0.35} | 92.93 _{0.61} | 31.55 _{0.00} | 33.39 _{1.09} | 27.89 _{0.00} |
| | DC | 54.80 | 32.31 _{0.33} | 32.79 _{3.07} | 62.94 _{0.85} | 85.17 _{2.62} | 94.54 _{0.80} | 92.15 _{0.49} | 31.55 _{0.00} | 33.81 _{1.16} | 27.89 _{0.00} |
| | BC | 61.22 | 24.82 _{1.23} | 41.11 _{1.87} | 63.41 _{0.84} | 81.51 _{1.55} | 93.40 _{0.58} | 92.46 _{0.53} | 56.01 _{6.53} | 33.64 _{1.15} | 64.57 _{0.98} |
| | SC | 74.58 | 45.92 _{3.25} | 62.50 _{3.97} | 87.42 _{1.83} | 85.98 _{4.47} | 94.02 _{1.88} | 91.07 _{2.32} | 67.94 _{10.40} | 64.08 _{4.31} | 72.34 _{2.92} |

Table 6: Average Accuracy scores (%) for various calibration methods on selected datasets, evaluated for each LLM in the 4-shot setting ($k = 4$) over five random seeds. Values are presented as mean_{standard deviation}, with the highest score in each column highlighted in **bold** and shaded gray.

| Model | Method | Avg | AGNews | FPB | SST2 | RT | Subj | TE-Emo | TE-Hate |
|---------|----------|--------------|------------------------------|------------------------------|------------------------------|------------------------------|------------------------------|-------------------------------|------------------------------|
| Qwen | Base LLM | 68.01 | 75.23 _{1.61} | 63.36 _{2.91} | 87.93 _{7.44} | 88.28 _{1.85} | 48.16 _{0.38} | 56.41 _{1.52} | 56.68 _{0.08} |
| | CC | 64.34 | 85.47 _{4.80} | 50.94 _{13.11} | 91.99 _{0.67} | 89.92 _{1.35} | 51.09 _{4.15} | 37.58 _{8.27} | 43.36 _{0.00} |
| | DC | 65.87 | 88.91 _{0.58} | 52.73 _{10.46} | 87.30 _{5.81} | 90.31 _{0.90} | 50.04 _{1.74} | 48.44 _{3.54} | 43.36 _{0.00} |
| | BC | 74.71 | 78.28 _{1.53} | 76.64 _{2.85} | 89.06 _{3.53} | 90.20 _{1.41} | 74.30 _{3.84} | 57.85 _{1.53} | 56.64 _{0.00} |
| | SC | 70.62 | 77.34 _{3.89} | 74.69 _{9.28} | 90.82 _{4.17} | 89.41 _{1.74} | 65.82 _{8.12} | 45.08 _{20.38} | 51.17 _{6.97} |
| Llama | Base LLM | 72.86 | 82.58 _{4.17} | 78.55 _{2.69} | 93.63 _{0.40} | 91.17 _{1.58} | 51.88 _{7.02} | 72.85 _{5.23} | 46.33 _{3.47} |
| | CC | 71.40 | 79.30 _{2.02} | 85.51 _{2.17} | 93.48 _{0.94} | 92.07 _{0.95} | 47.85 _{0.00} | 58.20 _{0.92} | 43.36 _{0.00} |
| | DC | 71.47 | 79.61 _{1.89} | 85.94 _{2.33} | 93.83 _{1.19} | 91.95 _{1.18} | 47.85 _{0.00} | 57.77 _{1.35} | 43.36 _{0.00} |
| | BC | 74.05 | 77.19 _{1.27} | 86.99 _{3.09} | 93.75 _{0.48} | 91.52 _{1.28} | 58.20 _{3.41} | 58.24 _{1.68} | 52.46 _{1.97} |
| | SC | 73.78 | 78.12 _{8.67} | 86.29 _{2.88} | 94.45 _{0.47} | 91.56 _{1.18} | 56.45 _{10.80} | 61.05 _{14.12} | 48.52 _{1.90} |
| Mistral | Base LLM | 76.98 | 82.50 _{4.17} | 90.47 _{1.99} | 94.22 _{0.76} | 92.50 _{0.62} | 53.91 _{0.00} | 68.36 _{5.16} | 56.88 _{7.72} |
| | CC | 69.56 | 75.23 _{2.33} | 87.34 _{1.57} | 94.92 _{0.70} | 92.42 _{0.72} | 46.09 _{0.00} | 52.27 _{2.13} | 38.67 _{0.00} |
| | DC | 69.44 | 75.31 _{1.81} | 85.86 _{3.40} | 94.38 _{0.19} | 92.42 _{0.72} | 46.09 _{0.00} | 53.36 _{2.16} | 38.67 _{0.00} |
| | BC | 73.21 | 74.69 _{1.57} | 87.19 _{2.28} | 94.14 _{0.70} | 92.66 _{0.67} | 48.44 _{9.55} | 53.13 _{1.40} | 62.27 _{2.35} |
| | SC | 75.59 | 80.23 _{9.04} | 92.50 _{1.87} | 95.23 _{1.09} | 91.56 _{1.45} | 62.03 _{8.98} | 65.23 _{14.12} | 42.27 _{17.35} |

Table 7: Average Accuracy scores (%) for various calibration methods on selected datasets, evaluated for each LLM in the 8-shot setting ($k = 8$) over five random seeds. Values are presented as mean_{standard deviation}, with the highest score in each column highlighted in **bold** and shaded gray.

| Model | Method | Avg | SST5 | TREC | AGNews | FPB | SST2 | RT | Subj | TE-Emo | TE-Hate |
|---------|----------|--------------|------------------------------|------------------------------|------------------------------|------------------------------|------------------------------|------------------------------|------------------------------|-------------------------------|------------------------------|
| Qwen | Base LLM | 60.32 | 24.34 _{0.16} | 54.22 _{7.21} | 73.16 _{0.81} | 62.58 _{0.52} | 76.09 _{16.30} | 91.02 _{2.26} | 46.09 _{0.00} | 54.06 _{2.74} | 61.33 _{0.00} |
| | CC | 58.59 | 24.26 _{0.08} | 67.34 _{3.93} | 83.98 _{4.99} | 33.28 _{6.70} | 89.53 _{2.29} | 92.30 _{1.37} | 46.64 _{0.47} | 51.33 _{7.54} | 38.67 _{0.00} |
| | DC | 55.94 | 24.26 _{0.08} | 52.81 _{1.70} | 87.27 _{0.79} | 33.13 _{4.34} | 71.72 _{16.75} | 91.09 _{1.48} | 47.66 _{2.05} | 56.88 _{3.25} | 38.67 _{0.00} |
| | BC | 68.64 | 24.30 _{0.10} | 73.59 _{1.79} | 74.65 _{0.69} | 70.70 _{3.10} | 86.52 _{4.48} | 91.95 _{1.40} | 77.03 _{1.34} | 57.66 _{1.63} | 61.33 _{0.00} |
| | SC | 72.30 | 43.52 _{4.28} | 69.06 _{1.32} | 86.02 _{4.01} | 76.33 _{6.70} | 91.88 _{3.27} | 90.70 _{2.46} | 72.50 _{3.45} | 61.33 _{20.50} | 59.38 _{3.81} |
| Llama | Base LLM | 66.62 | 23.12 _{0.67} | 56.88 _{4.73} | 80.08 _{2.99} | 84.14 _{3.44} | 94.30 _{1.12} | 91.95 _{1.17} | 48.75 _{3.30} | 75.39 _{3.59} | 45.00 _{5.04} |
| | CC | 63.59 | 50.08 _{3.00} | 36.48 _{3.58} | 76.09 _{1.24} | 82.73 _{3.44} | 94.77 _{0.72} | 92.42 _{0.72} | 46.09 _{0.00} | 55.00 _{2.06} | 38.67 _{0.00} |
| | DC | 63.71 | 48.59 _{3.28} | 37.66 _{3.71} | 76.80 _{0.88} | 84.06 _{2.90} | 94.61 _{1.29} | 92.50 _{0.63} | 46.09 _{0.00} | 54.37 _{1.86} | 38.67 _{0.00} |
| | BC | 66.55 | 31.48 _{1.37} | 47.50 _{1.69} | 75.78 _{1.64} | 83.44 _{3.69} | 94.22 _{1.38} | 92.03 _{1.04} | 65.78 _{4.30} | 54.77 _{1.70} | 53.91 _{2.60} |
| | SC | 71.61 | 45.94 _{5.52} | 50.86 _{10.44} | 86.56 _{2.76} | 86.95 _{2.35} | 95.39 _{0.52} | 92.58 _{1.24} | 63.05 _{3.39} | 73.52 _{4.08} | 49.61 _{3.55} |
| Mistral | Base LLM | 68.27 | 23.05 _{0.25} | 51.48 _{5.31} | 76.88 _{1.66} | 85.86 _{5.64} | 94.53 _{1.75} | 92.66 _{0.46} | 54.84 _{1.88} | 74.30 _{1.84} | 60.86 _{5.49} |
| | CC | 64.42 | 54.22 _{0.52} | 40.86 _{3.51} | 74.45 _{1.67} | 84.61 _{5.70} | 94.38 _{1.76} | 92.73 _{0.40} | 46.09 _{0.00} | 53.75 _{1.69} | 38.67 _{0.00} |
| | DC | 65.02 | 54.06 _{0.72} | 43.36 _{3.44} | 74.30 _{0.62} | 86.64 _{5.28} | 94.84 _{1.51} | 92.73 _{0.47} | 46.09 _{0.00} | 54.45 _{1.25} | 38.67 _{0.00} |
| | BC | 66.35 | 34.92 _{0.53} | 51.48 _{4.13} | 73.67 _{1.12} | 83.91 _{4.18} | 94.30 _{1.51} | 92.66 _{0.67} | 48.75 _{7.86} | 53.67 _{1.76} | 63.83 _{1.86} |
| | SC | 75.54 | 48.52 _{5.84} | 57.58 _{8.88} | 87.42 _{3.19} | 89.53 _{5.11} | 93.59 _{1.41} | 90.16 _{1.68} | 67.50 _{6.08} | 75.16 _{5.08} | 70.39 _{6.96} |

Table 8: Average Accuracy scores (%) for various calibration methods on selected datasets, evaluated for each LLM in the 16-shot setting ($k = 16$) over five random seeds. Values are presented as mean_{standard deviation}, with the highest score in each column highlighted in **bold** and shaded gray.

| Model | Method | Avg | SST5 | TREC | AGNews | FPB | SST2 | RT | Subj | TE-Emo | TE-Hate |
|---------|----------|--------------|------------------------------|------------------------------|------------------------------|------------------------------|------------------------------|------------------------------|------------------------------|------------------------------|------------------------------|
| Qwen | Base LLM | 62.71 | 22.81 _{0.19} | 60.16 _{3.27} | 75.62 _{0.94} | 64.06 _{0.00} | 87.66 _{6.53} | 91.56 _{1.81} | 46.09 _{0.00} | 55.08 _{0.96} | 61.33 _{0.00} |
| | CC | 59.08 | 22.81 _{0.19} | 70.00 _{1.29} | 86.17 _{2.18} | 25.08 _{8.06} | 92.66 _{0.83} | 93.36 _{0.65} | 49.30 _{2.61} | 53.67 _{1.99} | 38.67 _{0.00} |
| | DC | 57.47 | 22.81 _{0.19} | 51.02 _{3.73} | 88.44 _{0.72} | 37.03 _{15.89} | 84.14 _{9.51} | 93.44 _{1.06} | 48.05 _{2.37} | 53.59 _{1.09} | 38.67 _{0.00} |
| | BC | 69.49 | 22.89 _{0.19} | 73.91 _{2.07} | 78.05 _{1.59} | 72.81 _{8.05} | 91.41 _{0.92} | 92.66 _{0.90} | 76.80 _{2.87} | 55.55 _{0.62} | 61.33 _{0.00} |
| | SC | 70.77 | 41.64 _{6.65} | 73.98 _{2.67} | 85.78 _{3.38} | 67.11 _{11.83} | 93.20 _{1.89} | 92.19 _{1.42} | 68.52 _{8.27} | 60.23 _{5.91} | 54.30 _{8.05} |
| Llama | Base LLM | 66.97 | 22.50 _{0.31} | 65.86 _{3.44} | 81.09 _{2.71} | 81.72 _{5.09} | 94.45 _{0.57} | 92.03 _{1.27} | 48.75 _{2.09} | 73.20 _{6.24} | 43.12 _{3.08} |
| | CC | 63.88 | 52.58 _{0.80} | 37.19 _{3.21} | 75.86 _{1.47} | 82.34 _{5.05} | 94.61 _{1.09} | 92.81 _{0.68} | 46.09 _{0.00} | 54.77 _{0.76} | 38.67 _{0.00} |
| | DC | 64.11 | 50.70 _{1.84} | 39.14 _{4.17} | 76.95 _{0.86} | 85.23 _{4.79} | 94.77 _{1.15} | 92.81 _{0.80} | 46.09 _{0.00} | 52.66 _{1.70} | 38.67 _{0.00} |
| | BC | 66.86 | 33.36 _{1.32} | 44.22 _{3.30} | 76.25 _{0.80} | 83.52 _{5.10} | 94.61 _{0.83} | 92.34 _{1.12} | 66.64 _{2.38} | 54.30 _{0.35} | 56.48 _{4.29} |
| | SC | 70.92 | 44.45 _{4.58} | 65.47 _{4.60} | 87.42 _{2.90} | 78.83 _{12.25} | 93.98 _{0.77} | 91.88 _{1.45} | 56.88 _{8.83} | 66.64 _{5.59} | 52.73 _{11.41} |
| Mistral | Base LLM | 67.65 | 22.73 _{0.16} | 56.88 _{4.99} | 78.67 _{1.92} | 83.91 _{3.73} | 93.98 _{0.80} | 92.42 _{0.72} | 55.08 _{1.44} | 76.48 _{3.62} | 48.67 _{6.38} |
| | CC | 64.57 | 54.30 _{0.55} | 42.66 _{4.30} | 75.78 _{1.05} | 82.03 _{3.38} | 94.06 _{0.38} | 92.97 _{0.61} | 46.09 _{0.00} | 54.53 _{1.74} | 38.67 _{0.00} |
| | DC | 65.41 | 54.14 _{0.72} | 47.11 _{4.27} | 75.47 _{1.03} | 85.08 _{3.46} | 94.69 _{0.80} | 92.19 _{0.49} | 46.09 _{0.00} | 55.23 _{1.76} | 38.67 _{0.00} |
| | BC | 67.52 | 34.69 _{1.32} | 53.28 _{2.16} | 75.94 _{1.01} | 81.25 _{2.14} | 93.52 _{0.58} | 92.50 _{0.52} | 56.56 _{6.32} | 55.00 _{1.81} | 64.92 _{0.90} |
| | SC | 76.96 | 47.27 _{2.43} | 73.28 _{3.01} | 87.81 _{1.81} | 85.78 _{6.80} | 94.30 _{1.70} | 91.09 _{2.34} | 70.86 _{7.29} | 68.05 _{5.05} | 74.22 _{1.38} |

H Ablation results

We conduct ablation studies to dissect the distinct contributions of key components within our Supervised Calibration (SC) framework.

First, to isolate the impact of learning the per-class scaling factor w_c , which underpins SC’s ability to reorient decision boundaries, we compare the full SC model against two alternatives: a restricted variant, SC* (where w_c is fixed to 1, thus only learning an optimal bias term), and other baseline calibration methods. Our experiments reveal that SC* surpasses these other baselines. This suggests that estimating an optimal bias under SC framework is more effective than methods employed by LM methods. More critically, the full SC model achieves higher performance than SC*, suggesting that the flexibility to learn the scaling factor—and therefore to both shift and rescale the LLM’s logits—offers a further advantage.

Second, we investigate whether aggregating calibrators trained with different context sizes improves predictive performance. Concretely, we train a collection of models $\{\hat{\theta}^i\}_{i \in I}$, where each calibrator is fitted using training data with i in-context examples. We then ensemble these context-size-specific calibrators and evaluate the impact of increasing the number of distinct i -shot learners in the ensemble (i.e., increasing $|I|$). Empirically, we observe a consistent and monotonic improvement in both Accuracy and Macro-F1 scores as $|I|$ grows. This suggests that calibrators exposed to heterogeneous amounts of contextual information offer complementary signals, enhancing the robustness and predictive accuracy of the final calibrated output. These findings highlight a promising direction: with sufficient computational resources, one could train and ensemble an even broader set of context-specific calibrators to capture a richer diversity of contextual patterns, potentially unlocking further performance gains.

Third, we investigate the impact of the number of sampled sub-contexts (m_i) used for prediction averaging within each context-size-specific calibrator during the ensembling phase. Our findings reveal that increasing m_i —that is, averaging predictions over a greater number of distinct sub-contexts of size i —generally enhances Macro-F1 scores. This suggests that more comprehensive sampling of available context variations for each i -shot learner improves the accuracy of the ensemble’s output, helping to further reduce ICL’s sensitivity to specific context compositions.

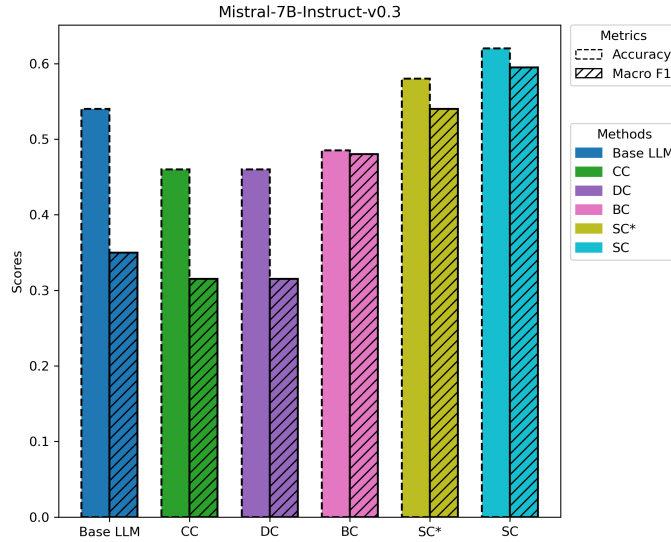


Figure 5: Accuracy and Macro-F1 scores of six methods on the Subjective dataset using the Mistral-7B-Instruct-v0.3 model in a 4-shot setting. Results are averaged over 5 random seeds. Bars represent the mean performance for each metric as indicated in the legend. SC* stands for the case where the scaling factor w_c is fixed to 1 under the SC framework. Notably, SC consistently outperforms all other methods. The improved performance of SC* over other baselines suggests that estimating an optimal bias under SC framework is more effective than the methods employed by LM approaches, while the full SC further demonstrates the advantage of also learning the scaling factor.

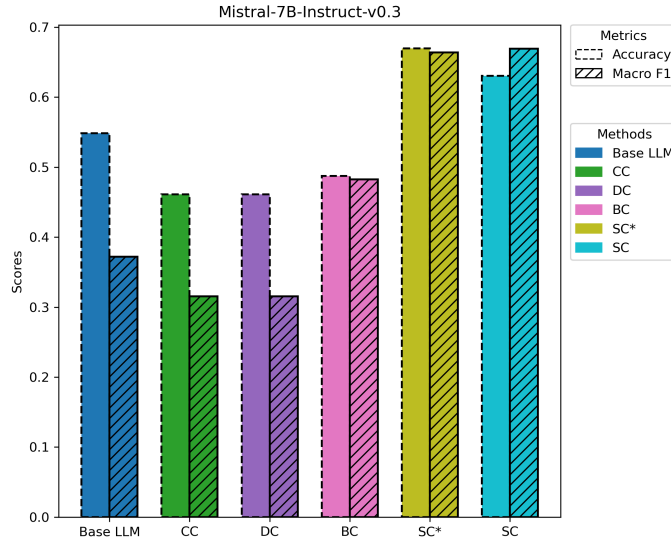


Figure 6: Accuracy and Macro-F1 scores of six methods on the Subjective dataset using the Mistral-7B-Instruct-v0.3 model in an 8-shot setting. Results are averaged over 5 random seeds. Bars represent the mean performance for each metric as indicated in the legend. SC* stands for the case where the scaling factor w_c is fixed to 1 under the SC framework. Notably, SC consistently outperforms all other methods. The improved performance of SC* over other baselines suggests that estimating an optimal bias under SC framework is more effective than the methods employed by LM approaches, while the full SC further demonstrates the advantage of also learning the scaling factor.

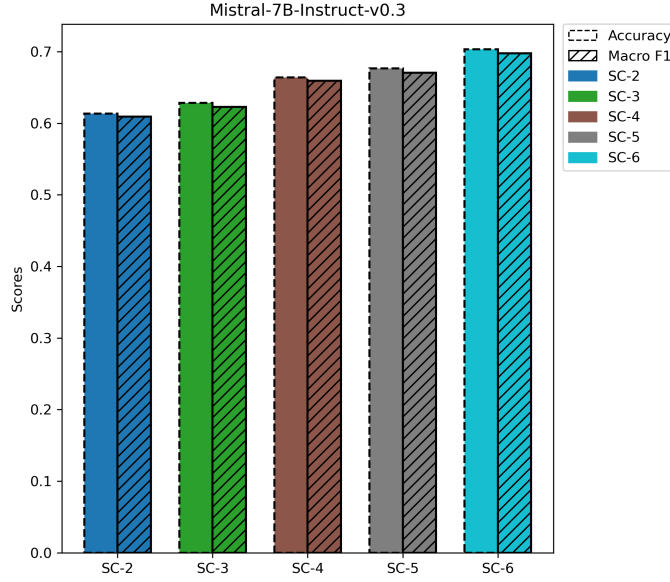


Figure 7: Impact of ensembling context-size-specific models within the SC framework on the Subjective dataset in an 8-shot setting. Result is reported for Mistral-7B-Instruct-v0.3, using Accuracy and Macro-F1 scores averaged over 5 random seeds. Each ensemble, denoted SC- N , aggregates calibration models trained on context sizes ranging from 1 to N (e.g., SC-2 uses models with context sizes 1 and 2, SC-6 includes context sizes 1 through 6). The consistent improvement in performance as N increases across all three LLMs highlights the general benefit of aggregating insights from a more diverse set of k -shot learners.

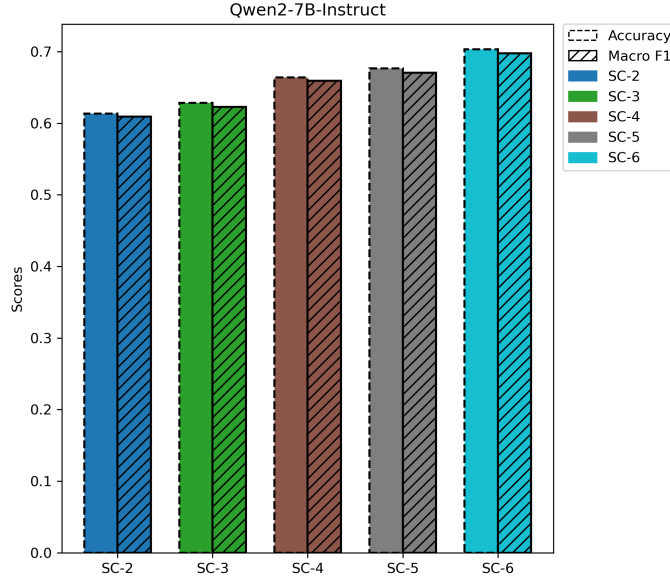


Figure 8: Impact of ensembling context-size-specific models within the SC framework on the Subjective dataset in an 8-shot setting. Results is reported for Qwen2-7B-Instruct, using Accuracy and Macro-F1 scores averaged over 5 random seeds. Each ensemble, denoted SC- N , aggregates calibration models trained on context sizes ranging from 1 to N (e.g., SC-2 uses models with context sizes 1 and 2, SC-6 includes context sizes 1 through 6). The consistent improvement in performance as N increases across all three LLMs highlights the general benefit of aggregating insights from a more diverse set of k -shot learners.

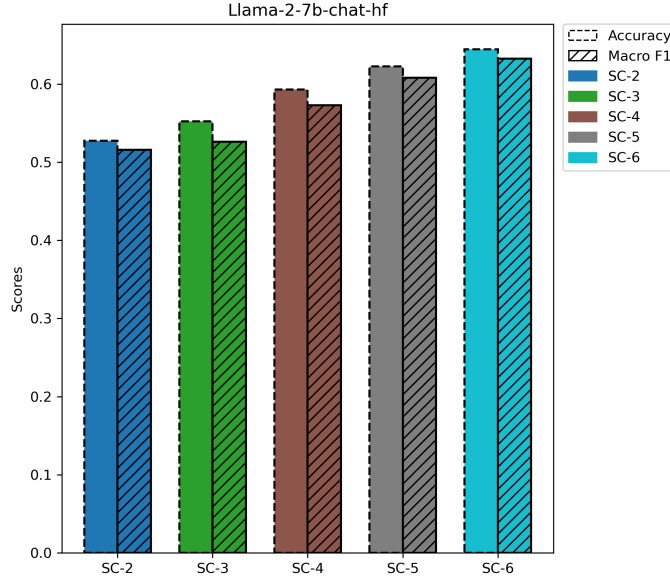


Figure 9: Impact of ensembling context-size-specific models within the SC framework on the Subjective dataset in an 8-shot setting. Result is reported for Llama-2-7b-chat-hf, using Accuracy and Macro-F1 scores averaged over 5 random seeds. Each ensemble, denoted SC- N , aggregates calibration models trained on context sizes ranging from 1 to N (e.g., SC-2 uses models with context sizes 1 and 2, SC-6 includes context sizes 1 through 6). The consistent improvement in performance as N increases across all three LLMs highlights the general benefit of aggregating insights from a more diverse set of k -shot learners.

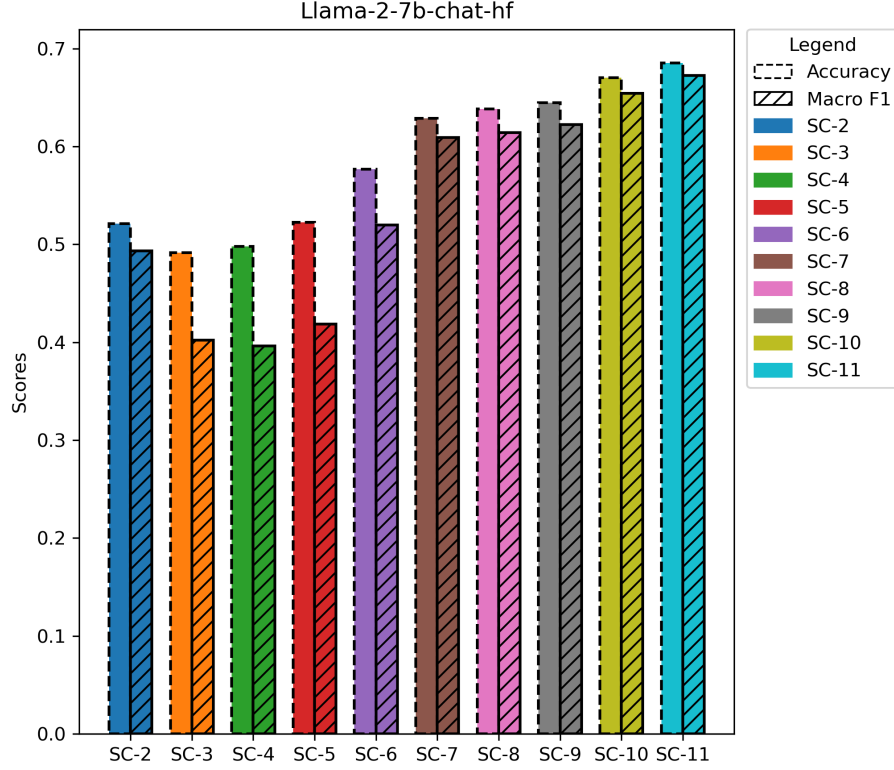


Figure 10: Impact of ensembling context-size-specific models within the SC framework on the Subjective dataset in an 16-shot setting. Result is reported for Llama-2-7b-chat-hf, using Accuracy and Macro-F1 scores averaged over 5 random seeds. Each ensemble, denoted SC- N , aggregates calibration models trained on context sizes ranging from 1 to N (e.g., SC-2 uses models with context sizes 1 and 2, SC-11 includes context sizes 1 through 11). The consistent improvement in performance as N increases across all three LLMs highlights the general benefit of aggregating insights from a more diverse set of k-shot learners.

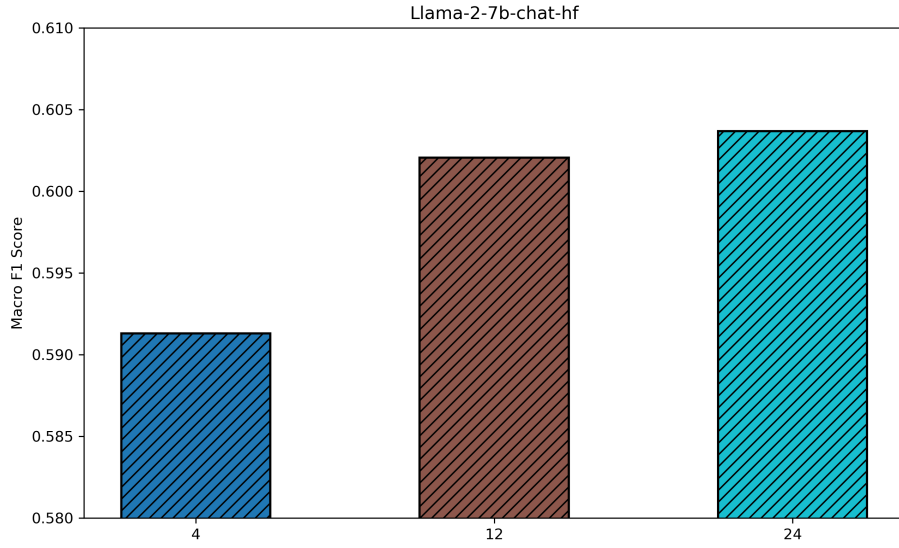


Figure 11: Impact of the number of sampled sub-contexts (m_i) used for prediction averaging within each context-size-specific model in the SC ensemble. Results show Macro-F1 scores on the Subjective dataset using the Llama-2-7b-chat-hf model in an 8-shot setting, averaged over 5 random seeds. The x-axis (m_i) represents the number of distinct contexts of a given size i sampled to generate predictions, which are then averaged. Performance improves as more context variations are considered in the ensemble prediction.